JACEP

Journal of Applied Civil Engineering and Practices

Online (e-ISSN): e-ISSN XXXX-XXXX || **Printed (p-ISSN)**: p-ISSN XXXX-XXXX
2025, Volume 1, No 1, pp.1-13

Evaluation of Intake Cofferdam Work Implementation Methods At the Muara Tawar PLTGU Project

Win Fauzi Ahmadi [a*], **Slamet Widodo** [b]

[a]Universitas Negeri Yogyakarta, Department of Civil Engineering, Faculty of Vocational, Indonesia
[b]Universitas Negeri Yogyakarta, Department of Civil Engineering and Planning Education, Faculty of Engineering, Indonesia

*Corresponding Author: winfauzi.2019@student.uny.ac.id

To cite this article:
Ahmadi W F, Widodo S (2025). Evaluation of Intake Cofferdam Work Implementation Methods At the Muara Tawar PLTGU Project. *Journal of Applied Civil Engineering and Practices*, 1(1), Pp 1-13.
doi: xx.xxxx/xxxxxx.xxxx.xxxxxx

To link to this article:
http://doi.org/ xx.xxxx/xxxxxx.xxxx.xxxxxx

Journal of Applied Civil Engineering and Practice by Department Bachelor of Applied Science in Civil Engineering, Faculty of Vocational, Universitas Negeri Yogyakarta.

2025, Volume 1, No 1, pp.1-13, e-ISSN XXXX-XXXX

JACEP

Journal of Applied Civil Engineering and Practice

Journal homepage: https://journal.uny.ac.id/publications/jacep/index

Research paper

Evaluation of Intake Cofferdam Work Implementation Methods At the Muara Tawar PLTGU Project

Win Fauzi Ahmadi [a*], **Slamet Widodo**[b]

[a]Universitas Negeri Yogyakarta, Department of Civil Engineering, Faculty of Vocational, Indonesia
[b]Universitas Negeri Yogyakarta, Department of Civil Engineering and Planning Education, Faculty of Engineering, Indonesia
*Corresponding Author: winfauzi.2019@student.uny.ac.id

ARTICLE INFO

Article History:
Received: March 14, 2025
Accepted: May 16, 2025
Published: May 20, 2025

Keywords:
Cofferdam, Intake, Stability

How To Cite:
Ahmadi W F, Widodo S (2024). Evaluation of Intake Cofferdam Work Implementation Methods At the Muara Tawar PLTGU Project. *Journal of Applied Nature and Construction*, 1(1), Pp 1-13. doi: xx.xxxx/xxxxxx.xxxx.xxxxxx

ABSTRACT

Purpose: The construction of a new intake in the Muara Tawar PLTGU must be carried out by demolishing the existing walls of the canal. There was a shift in the intake cofferdam in the Muara Tawar PLTGU project which caused a delay in the duration of the work so that the contractor suffered losses. The evaluation of the implementation method of the intake cofferdam work aims to analyze the existing stability conditions in several conditions against shear and overturning, analyze the safety of the existing profile, redesign the cofferdam so that it does not experience a shift, and propose a new method of installing the cofferdam.

Methods/Design: The evaluation method was carried out by collecting data based on field observations and interviews with four existing conditions: (1) Cofferdam flooding due to seepage; (2) Flooding due to tides; (3) Conditions if the cofferdam is fully installed; (4) Flooding due to rain. Data analysis techniques accordance with SNI 03-1729-2000 Specifications for Structural Steel Buildings.

Findings: The evaluation results show that the intake cofferdam at the Muara Tawar PLTGU has shifted due to the absence of locks on other buildings. The shift value is obtained from the calculation of shear stability ≤ 1.5. In terms of overturning moment stability, the cofferdam experienced overturning because the overturning moment stability value ≤ 1.5. The cofferdam structure bar force fulfills in resisting the forces that occur in the cofferdam.

Practical implication: With the shift, a redesign is carried out, namely adding anchor locks to 12 joints using mechanical anchors with each baseplate using 2 22 mm diameter anchors.

INTRODUCTION (1 – 2 pages)

Muara Tawar Combine Cycle Power Plan 2, 3, & 4 Add On 650 Project is the name of the project to add 3 electricity production blocks. The project is worth IDR 2,109 billion with the contractor PT. Hutama Karya and Doosan Heavy. The PLTGU production system requires two main fuel sources to carry out production. The fuel for electricity production at PLTGU is gas and water. PLTGU Muara Tawar collaborates with the state gas company to fulfil gas as the main ingredient for electricity production. Meanwhile, water is obtained from the sea and will be processed. The entry of sea water will be through the Circulating Water Intake (CW Intake) building. The CW Intake add-on project was built by demolishing the existing retaining wall. CW Intake blocks 2, 3 and 4 will be built next to CW Intake block 1 and block 5 which are already actively producing electricity. All additional buildings for blocks 2, 3 and 4 were made similar to blocks 1 and 5 with the same layout. Construction starting from the Balance of Plant (BOP) and Power Block is still in one area and adjacent to other blocks. CW Intake is built on an existing canal with a concrete-based canal floor. For this reason, appropriate work methods are needed for the construction of add on CW Intake blocks 2, 3 and 4.

Figure 1. Cofferdam Shift

As time increases, the use of the cofferdam method as protection against the destruction of existing retaining walls is experiencing problems. This obstacle is in the form of a shift in the position of the cofferdam due to tides. Shifting of the cofferdam causes leaks in the work area, disrupting the work of dismantling the existing wall. With the disruption of existing demolition work, the work had to be postponed and resulted in the contractor experiencing losses

The purpose of discussing these problems includes:

1. Determine the stability of shear forces and the stability of overturning moments that occur in the intake cofferdam of the Add on Block 2, 3 and 4 PLTGU Muara Tawar Project.
2. Know the security profile IWF 200.200.8.12 on the existing cofferdam.

3. Know an effective design so that the cofferdam does not shift.
4. Propose a new cofferdam installation method.

METHODS

The method used is to analyse the cofferdam in four conditions, namely the existing condition experiencing seepage, the existing condition experiencing flooding due to sea tides, the existing condition if it is installed perfectly, and the existing condition when flooding occurs due to rain. The initial stage of the study begins with a literature review which contains information on calculation standards and other information that can support the calculation analysis. The literature review was obtained from literature, lecture teaching materials, Indonesian National Standards (SNI 03-1729-2000), and journals regarding steel roof structures. After the calculation standards are determined, data in the form of image documents and other documents can be analysed. Analysis calculations use manual calculations and are assisted by FEM software. Several steps taken:

1. Collection of data related to cofferdam planning for the Muara Tawar PLTGU Project.
2. Determine the materials used in cofferdam construction and the loads that occur.
3. Structural calculation analysis was carried out by reviewing the structural components and cofferdam supports
4. Plan cofferdam redesign considering safety and equal loading.

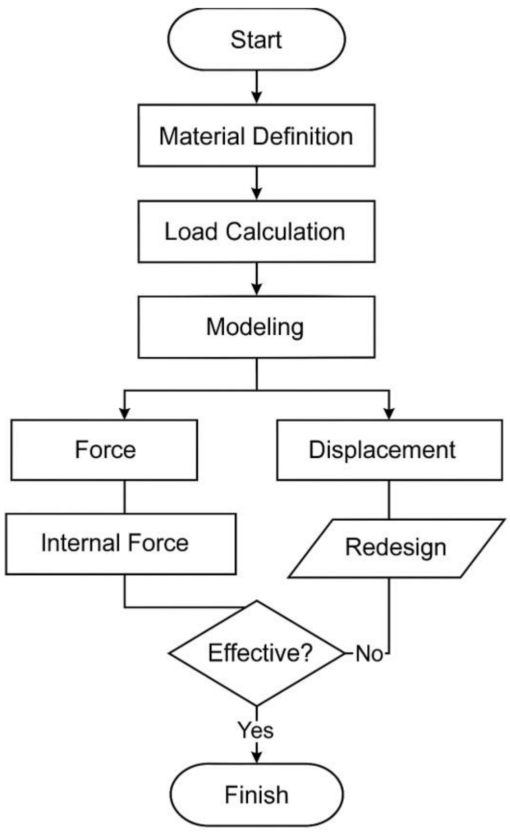

Figure 2. Flow Chart Data Analysis

Data analysis on the cofferdam structure is carried out in the following way:

1. Analyse the loads acting on the cofferdam structure and look for structural reactions due to the loads.
2. Calculating the sliding and overturning safety factors on existing cofferdams.
3. Plan appropriate and safe connections to lock the cofferdam to prevent shifting.
4. Plan methods that can be used for cofferdam installation work.

FINDINGS

1. Research Data

The material used for the cofferdam in the Muara Tawar PLTGU project is steel. The steel material used refers to JIS G3101 SS400 or ASTM A36. In JIS (Japanese Industrial Standard) SS400 is structural steel which has a grade of 400, while in ASTM (American Standard Testing and Material) the same steel is classified as grade 36. The weight of the cofferdam structure is 127.47 kN.

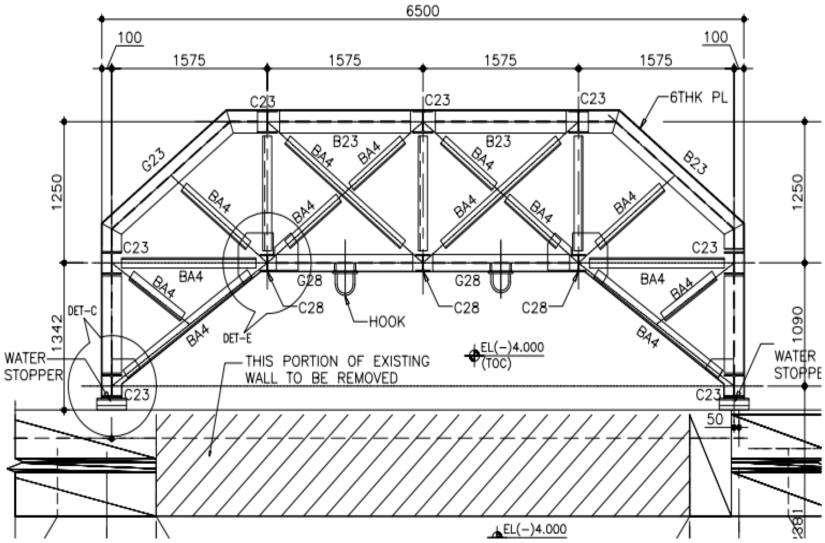

Figure 3. existing cofferdam design

Analysing drawings of the cofferdam structure on the Muara Tawar PLTGU project. The images reviewed include images of the existing canal walls, buildings around the cofferdam, and details of the cofferdam design.

Table 1. Data on the steel material used

Profile Steel Parts		Mark	Unit
Steel yield stress	(f_{yk})	245	MPa
Body height	(d_t)	200	mm
Wingspan	(b_f)	200	mm
Body thickness	(t_w)	8	mm
Wing thickness	(t_f)	12	mm

The cofferdam used is made from various types of steel profiles and steel plates as cofferdam walls. The steel profile refers to PT's steel product catalogue. Mount Garuda. The following types of steel are used in cofferdam structures.

Table 2. Dimension of Steel Profile

Type	Dimension		Weight
	H X B	A	
	mm	cm2	kg/m
IWF	200 x 200	63.53	49.9
IWF	150 x 150	40.14	31.5
Equal Angel	90 x 90	17	8.28

Furthermore, the water level has been measured based on four conditions and described based on the canal water level and the cofferdam water level on the table 3.

Table 3. The Water levels

Type	Dimensi		Weight
	H X B	A	
	mm	cm2	kg/m
IWF	200 x 200	63.53	49.9
IWF	150 x 150	40.14	31.5
Equal Angel	90 x 90	17	8.28

Apart from the cofferdam data, water level data in the canal was obtained PLTGU Muara Tawar in several conditions. Water level height at Channels can change according to natural conditions. This data is based on field observations and interviews conducted with workers in particular intake section. Several water level elevation conditions in the canal.

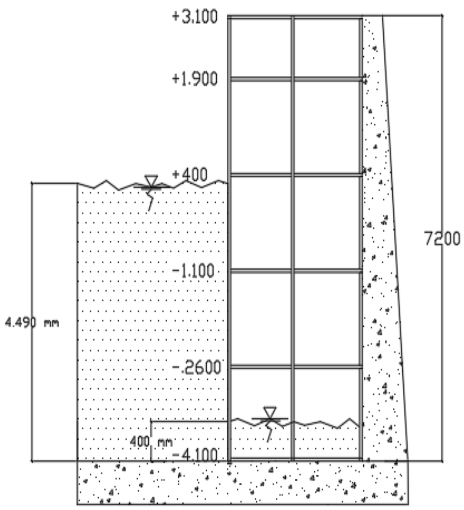

Figure 4. Water Level Height Condition 1

2. Shear and Roll Analysis

Analysis of existing conditions is carried out by calculating force or pressure which can affect the cofferdam structure. Because the cofferdam is in the canal or in direct contact with water, hydrostatic pressure will increase affect the cofferdam, in addition to the cofferdam hydrostatic pressure will also get the gravitational force. After all the compressive forces are calculated then It can be seen that the compressive force acting in the vertical direction is obtained from the weight cofferdam and horizontal compressive forces result from hydrostatic effects water in the cofferdam. These two pressing forces will be used for checking the stability of the cofferdam against shifting.

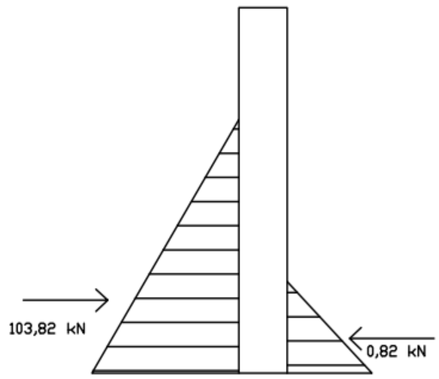

Figure 5. Direction of force in condition 1

The load that occurs on the cofferdam consists of the load due to the hydrostatic pressure of the water and the load on the cofferdam itself. Where the hydrostatics of water can be obtained from the following equation.

$$Pa = \frac{1}{2} \gamma h2 \quad (1)$$

To determine the stability of sliding, you can use the equation.

$$Sf = f \frac{\Sigma V}{\Sigma H} \quad (2)$$

Rolling stability is also calculated by:

$$F_{gl} = \frac{M_w}{M_g} \quad (3)$$

The safety value for sliding and rolling stability is declared safe if it exceeds 1.5. Cofferdam hydrostatic pressure occurs so that the loading produces the following forces.

Table 4. Load

Condition	Active Load (Pa)	Passive Load (Pp)
1	103.82 kN	0.82 kN
2	185.4 kN	0.20 kN
3	103.82 kN	0 kN
4	144.66 kN	31.16 kN

By knowing all these forces, shear stability and rolling stability can be produced as in table 5

Table 5. Sliding and Rolling Stability

Condition	S_f	Description	F_{gl}	Description
1	0,37	*Unacceptable*	0,42	*Unacceptable*
2	0,2	*Unacceptable*	0,24	*Unacceptable*
3	0,36	*Unacceptable*	0,42	*Unacceptable*
4	0,33	*Unacceptable*	0,38	*Unacceptable*

3. Profile Strength Analysis

When planning a steel structure, you must pay attention to the strength of the steel rods used to carry the load that occurs. Calculation of the strength of steel bars can be done in the following way:

a. Calculation of nominal moments due to local buckling effects
   Compact cross section, l ≤ lp
   Mn = Mp
   Non-compact cross section, lp < l ≤ lr
   Mn = Mp - (Mp - Mr) . (l - lp) / (lr - lp)
   Slim cross section, l > lr
   Mn = Mr . (lr / l)2 (4)
b. Nominal moment of lateral buckling influence
   Short span: L ≤ Lp
   Mn = Mp = fy . Zx
   Medium span: Lp ≤ L ≤ Lr
   Mn = Cb . [Mr + (Mp - Mr) . (Lr - L) / (Lr - Lp)](8)
   Long span: L > Lr
   Mn = Cb.p/ L.√[E.Iy.G.J + (p . E / L)2 .Iy.Iw] (5)
c. Bending Moment Resistance
   Mux / (fb . Mnx) + Muy / (fb . Mny) ≤ 1.0 (6)
d. Shear Resistance
   Vux / (ff . Vnx) + Vuy / (ff . Vny) ≤ 1.0 (7)
e. Shear and Flexure Interaction
   Mu / (fb . Mn) + 0.625 . Vu / (ff . Vn) ≤ 1.375 (8)

After analyzing with FEM software, the largest bar force output is produced as follows.

(M_{ux}) =	133591847,7	Nmm
(M_{uy}) =	131759963,1	Nmm
(V_{ux}) =	167627	N
(V_{uy}) =	162085	N

The rod style in the IWF 200.200.8.12 profile used for the cofferdam can be concluded that the profile has a compact flange, including a short span and adequate shear resistance. The above review concluded that the profile is safe. Apart from that, the results of the shear and bending interaction control calculations meet the requirements. With this, the cross-section of the cofferdam profile does not need to be redesigned. The following are the results of the IWF 200.200.8.12 rod force analysis on the existing cofferdam profile.

Table 6. IWF Profile strength 200.200.8.12

No	Reaction	Result	Information
1	Bending moment	0.43	OK
2	Shear resistance	0.92	OK
3	Shear and bending interactions	0.82	OK

4. Anchor Planning

Anchor connection planning refers to (SNI 03-1729-2000) Specifications for Structural Steel Buildings. Planning the connection can be done using the LRFD method.

a. Concrete bearing resistance

$$q = \frac{Pu}{Y} \quad (9)$$

b. Support plate thickness

$$q = \frac{Pu}{Y}$$

c. Bolt pulling force

$$T_u = (q_{max}.Y) - P_u \quad (10)$$

d. Bolt shear force

$$V_{u1} = \frac{V_U}{n} \quad (11)$$

e. Combination of drag and slide

$$F_{nt} = 0{,}75 + fu^b \quad (12)$$

$$F_{nv} = 0{,}45 + fu^b \quad (13)$$

f. Anchor support resistance

$$R_n = 2{,}4 . d . t . fu^p \quad (14)$$

The cofferdam shift occurred because there was no locking of the cofferdam with other buildings around it. Due to this, design improvements are needed to prevent the cofferdam from shifting. Effective cofferdam design planning by locking using anchors on the cofferdam profile and existing walls. The cofferdam shift value is high because the modeling uses a two-point joint approach by looking at shifts in the X and Y directions, so anchor planning will be carried out on 12 joints with existing conditions experiencing flooding due to sea tides. After modelling in FEM software, the force, displacement and moment values are obtained that Pu = 20.545,05 N, Mu = 17.956.284 Nmm and Vu = 25,492,99 N

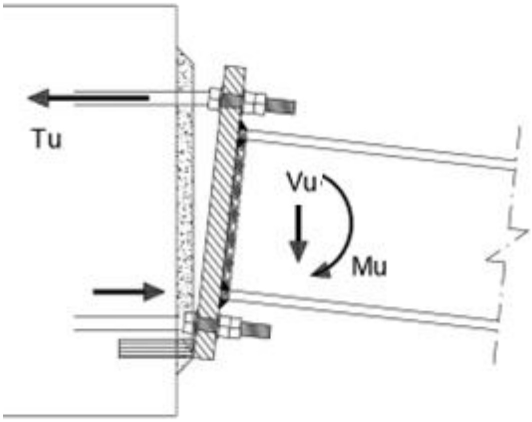

Figure 6. Illustration of Bolt Support

The anchor used is a mechanical anchor type. The use of mechanical anchors is to shorten installation time so that it is more efficient and has anchor strength that can bond with concrete walls. The anchor used is a strong bolt wedge anchor type measuring 19 mm in diameter and 200 mm long in accordance with the specifications in the Simpson Strong-Tie anchor factory catalogue. The following is the planning data for the anchor bolts used on the Table 7. The results of anchor planning using anchors with a diameter of 19 mm produce the Table 8.

Table 7. Planning data for the bolt anchors used

Category	Result
Steel yield stress	454 MPa
Plate breaking tensile stress	862 MPa
Anchor diameter	19 mm
Number of threads per inch	10 mm
Anchor length	200 mm
Plate/washer ring thickness	30 mm
Number of pressure side bolt anchors	1 pc
Number of pull side bolt anchors	1 pc
Number of rows of x direction bolt anchors	1
Number of rows of x direction bolt anchors	1

Table 8. The results of anchor planning using anchors

No	Force	Occurring Force	Maximum Design Strength	Note
1	Concrete support pressure	2850 N/mm	8425.63 N/mm	OK
2	Tensile force	40.189 N	138.629 N	OK
3	Shear force	12.746 N	73.304 N	OK
4	Combination of shear and tension	325.72 MPa	484.76 MPa	OK
5	Bolt anchor style	12.746.5 N	379.620	OK

From the results above, it can be concluded that the locking plan using anchors with a diameter of 19 mm is safe. Locking with anchors according to the plan on the baseplate and anchor requirements can be seen in the Table 9.

Table 9. Locking with anchors according to plan

No	Baseplate Point	Number of anchors	Anchor Diameter
1	10	2	19
2	18	2	19
3	135	2	19
4	143	2	19
5	117	2	19
6	126	2	19
7	99	2	19
8	107	2	19
9	83	2	19
10	91	2	19
11	58	2	19
12	66	2	19

5. Implementation Method

a. Make a mud pool

Making mud pools is done by excavating the soil around the cofferdam work. Excavation using a PC 78 excavator is easy to do. The dimensions of the pond and the depth of the excavation depend on the area where the cofferdam will be placed. This excavation aims to accommodate mud and sand deposits at the bottom of the canal in the cofferdam area.

b. Assemble Tripod Crane

The tripod crane is installed on the concrete floor of the CWPH (Circulation Water Pump House) building. Narrow access means that the tripod crane segment must be transported using a tower crane. Transport to the location according to the segments to be assembled. The assembly is done manually with the help of hand tools. After the tripod crane circuit is installed, connect the electricity to the generator.

c. Cofferdam Area Cleaning

The base of the canal floor must be cleaned of material. Material cleaning within a 15-meter radius around the cofferdam area. The aim of cleaning is at a distance of 15 meters so that waste material carried by water currents does not end up in the cofferdam area. The main object in cleaning activities is waste material with large dimensions. For example, leftover building materials that are under water, wood waste, plastic waste with large dimensions and coral that is attached to existing walls. Coral residue from plants and aquatic animals attached to existing walls must be cleaned thoroughly.

d. Dredging

Mud and sand at the bottom of the canal will affect the performance of the cofferdam. Therefore, dredging activities are needed. Dredging activities aim to remove mud and sand from the bottom of the canal in the cofferdam placement area by moving the mud and sand at the bottom of the canal to a storage or sediment pond. Dreging is done by sucking up mud and sand using a high capacity pump on a simple boat and then channeling it using an HDPE pipe to a holding pond.

e. Lifting Cofferdam

After the tripod crane and cofferdam have been rubberized on the part that will stick to the concrete, lift the cofferdam using a tripod crane. The cofferdam placement process is placed according to the planned point. Lower the cofferdam and try to make contact with the existing wall. The lowering process is carried out slowly and carefully. The rigger and operator must work together so that the cofferdam matches the point that the surveyor has made.

f. Close the canal floodgates

The closure of the canal sluice gates is carried out at the same time as the lifting of the cofferdam so that the closing time of the canal sluice gates and the work can be completed in less than 3 hours. Closing the sluice gate if done for more than 3 hours will of course affect the electricity production of other blocks that are already active. Therefore, workers installing scaffolding and workers tasked with installing anchors must be ready.

g. Put up scaffolding

Scaffolding is made of iron pipes strung above the water surface. Scaffolding is installed by lowering the scaffolding using a tower crane. Installation of scaffolding according to both sides of the cofferdam where anchorage will be carried out. The size of the scaffolding is also adjusted to the position of the anchor installation.

h. Installation of anchors

Installation of steel anchors must be done in the right way and in a short time. The anchor installation was carried out by four groups, namely the inner anchor installation group (2 groups) and the outer cofferdam installation group (2 groups). Installation is carried out at two points together, starting from the bottom anchor then moving to the top point.

Based on the application results of the temporary cofferdam in the Shenzhen–Zhongshan river channel, it is found that the overall stability and overturning stability of the cofferdam meet the relevant safety requirements, with minimum safety factors of 1.744 and 1.400, respectively. The maximum displacement of the inner and outer steel piles is 34 mm, the maximum bending moment is 249.30 kN m, and the maximum shear force is 266.66 kN. The pile displacement is within the acceptable range, and the internal force remains below the load capacity of the pile type selected for design. (Jiang et all, 2023)

The boundary balance design theory is used to calculate the load limits on the cofferdam, considering the core fill of the dam and the sheet piles on both sides as a medium and a continuous elastic shell, while also analyzing the deformation based on various boundary conditions. (Buhan et al, 1996) A simplified two-dimensional (2D) model has been developed to analyze the structure of the steel sheet pile cofferdam and to investigate the characteristics of force deformation during construction according to the calculation program they developed (Lefas et al, 2001) The failure of a double-row steel sheet pile cofferdam has been analyzed using finite element software and low tie weld strength was identified as the cause of damage to the structure (Gui et al, 2009)

Steel piles have a rich history and have undergone significant development in Europe and Japan since their introduction in the early 20th century. These piles have been widely used in various construction applications, including dams, foundation supports at docks, bridges, underground tube tunnels, and other projects. Steel piles offer many advantages such as high quality, simple construction, durability, and the ability to reduce space requirements for construction tasks (Yang et al, 2020; Wu et al, 2023)

CONCLUSION

The results of the review of analytical calculations and discussion regarding the evaluation of the PLTGU Muara Tawar cofferdam, it can be concluded that: Existing cofferdam from seepage conditions, flood conditions due to sea tides, conditions if the cofferdam is installed perfectly, and flood conditions due to rain change with cofferdam shear stability value ≤ 1.5. Judging from the rolling stability, the cofferdam experienced overturning because the rolling stability value of the cofferdam in four conditions was ≤ 1.5. The results of the IWF 200.200.8.12 steel profile bar force calculation used are short spans with adequate shear resistance. In addition, the control of the shear and bending interactions that occur meets the requirements. Thus, the existing steel cofferdam cross-section does not need to be redesigned. Redesign of the cofferdam was carried out to resist shifting by using anchor locking connections on the existing canal walls so that the cofferdam does not shift. There are 12 baseplate points with each baseplate using 2 anchors with a diameter of 19 mm. The proposed method for carrying out cofferdam work includes creating mud pools, assembling tripod cranes, cleaning, dredging, lifting, closing canal sluice gates, installing scaffolding and installing anchors.

DISCLOSURE STATEMENT

contains statements that guarantee and ensure that there is no potential conflict of interest from the author.

REFERENCES

Badan Standardisasi Nasional. (2017). *SNI 03-1729-2000: Tata cara perencanaan struktur baja untuk bangunan gedung*. Badan Standardisasi Nasional.

Gui, M.-W.; Han, K.-K. (2009). An investigation on a failed double-wall cofferdam during construction. *Engineering Failure Analysis*, 16 (1), 421–432. https://doi.org/10.1016/j.engfailanal.2008.06.004.

Jiang, Y., Guo, F., Wang, W., Yang, G., Yue, J., Huang, Y. (2023). Stability Study of a Double-Row Steel Sheet Pile Cofferdam Structure on Soft Ground. *Water,* 15 (2643), 1-16. https://doi.org/10.3390/w15142643

Lefas, I., Georgiannou, V. (2001). Analysis of a cofferdam support and design implications. Computers & Structures., 79 (26), 2461–2469. https://doi.org/10.1016/S0045-7949(01)00082-7

Simpson Strong-Tie. (2016). *Product catalog*. Simpson Strong-Tie Company Inc.

Wu, S., Hao, W., Yao, Y., & Li, D. (2023). Investigation into durability degradation and fracture of cable bolts through laboratorial tests and hydrogeochemical modelling in underground conditions. *Tunnelling and Underground Space Technology, 138* (105198). https://doi.org/10.1016/j.tust.2023.105198

Yang, Y., Liu, W., Hu, A., Li, F., & Yang, Z. (2020). Application of steel sheet pile in deep foundation pit support of collapsible loess regions. *IOP Conference Series: Earth and Environmental Science, 474*(7), 072058. https://doi.org/10.1088/1755-1315/474/7/072058

JACEP

Journal of Applied Civil Engineering and Practices

Online (e-ISSN): e-ISSN XXXX-XXXX || **Printed (p-ISSN)**: p-ISSN XXXX-XXXX
2025, Volume 1, No 1, pp.14-26

Utilization of Recycled Asphalt with the Addition of Crushed Stone Ash as a Lataston Mixture for Flexible Pavement Construction: Case Study of Dredging Old Pavement on Jalan Wates Street KM 12

Loris Capirossi Suis [a*], **Dian Eksana Wibowo**[b]

[a]Universitas Negeri Yogyakarta, Department of Civil Engineering, Faculty of Vocational, Indonesia
[b]Universitas Negeri Yogyakarta, Department of Civil Engineering and Planning Education, Faculty of Engineering, Indonesia
*Corresponding Author: loriscapirossi.2019@student.uny.ac.id

To cite this article:
Suis L C, Wibowo D E (2025). Utilization of Recycled Asphalt with the Addition of Crushed Stone Ash as a Lataston Mixture for Flexible Pavement Construction: Case Study of Dredging Old Pavement on Jalan Wates Street KM 12. *Journal of Applied Civil Engineering and Practices*, 1(1), Pp 14-26. doi: xx.xxxx/xxxxxx.xxxx.xxxxxx

To link to this article:
http://doi.org/ xx.xxxx/xxxxxx.xxxx.xxxxxx

Journal of Applied Civil Engineering and Practice by Department Bachelor of Applied Science in Civil Engineering, Faculty of Vocational, Universitas Negeri Yogyakarta.

2025, Volume 1, No 1, pp.14-26, e-ISSN XXXX-XXXX

Journal of Applied Civil Engineering and Practice

Journal homepage: https://journal.uny.ac.id/publications/jacep/index

Research paper

Utilization of Recycled Asphalt with the Addition of Crushed Stone Ash as a Lataston Mixture for Flexible Pavement Construction: Case Study of Dredging Old Pavement on Jalan Wates Street KM 12

Loris Capirossi Suis [a*], **Dian Eksana Wibowo** [b]

[a]Universitas Negeri Yogyakarta, Department of Civil Engineering, Faculty of Vocational, Indonesia
[b]Universitas Negeri Yogyakarta, Department of Civil Engineering and Planning Education, Faculty of Engineering, Indonesia
*Corresponding Author: loriscapirossi.2019@student.uny.ac.id

ARTICLE INFO

Article History:
Received: March 16, 2025
Accepted: May 16, 2025
Published: May 23, 2025

Keywords:
Recycled Asphalt, Lataston Mixture, Flexible Pavement

How To Cite:
Suis L C, Wibowo D E (2025). Utilization of Recycled Asphalt with the Addition of Crushed Stone Ash as a Lataston Mixture for Flexible Pavement Construction: Case Study of Dredging Old Pavement on Jalan Wates Street KM 12. *Journal of Applied Civil Engineering and Practices*, 1(1), Pp 14-26. doi: xx.xxxx/xxxxxx.xxxx.xxxxxx

ABSTRACT

Purpose: The purpose of this study is to find the Optimum Asphalt Content in recycled asphalt, know the characteristics of marshall in recycled asphalt, and find out the flexibility and resistance in the use of recycled asphalt with the addition of crushed stone ash.

Methods/Design: The methods used in this study are experimental and qualitative. The research was conducted by utilizing asphalt waste (asphalt recycle) obtained from the results of road dredging on Jl. Wates, KM 12, Sedayu, Sleman, Yogyakarta.

Findings: Asphalt waste is substituted with asphalt pen 60/70 as a rejuvenating material and filler is added using crushed stone ash. The planned new asphalt mixture is with percentage variations of 2%, 2.5%, 3%, and 3.5%. Meanwhile, the ash content of crushed stone as a planned filler is 3%, 5%, and 7%. The optimum asphalt content (KAO) obtained on new asphalt for recycled asphalt mixture meets the specifications of the Hot Paved Mixture Layer Implementation Guidelines (2007) at 3% asphalt content, while for crushed stone ash as filler, the Optimum Asphalt Content (KAO) value is obtained at 5% crushed stone ash content. In the use of recycled asphalt for Lataston bending pavement with the addition of crushed rock ash to marshall parameters, Stability values of 1765.10 kg, Density 2.31 gr / cc, Flow 3.11 mm, and Marshall Qoutient 567.56 mm / kg were obtained

Practical implication: Utilization of asphalt recycling with the addition of ash Stone as a Lataston mixture for flexible pavement can improve the quality of flexible pavement by combining recycled asphalt and stone ash in the Lataston mixture. it can also contribute to improving road construction technology and practices, which can benefit the construction industry and society.

INTRODUCTION

Highway construction is very important to facilitate the smooth running of land transportation, therefore highway construction must be planned well in order to provide comfort and safety for vehicles passing on it. Roads are one of the land transportation infrastructures most widely used by people for daily activities, so the volume of land transportation traffic is higher compared to other modes of transportation such as water and air transportation. Therefore, road pavement must be designed to be able to bear the volume of vehicles passing on it. In general, road pavement construction can be divided into flexible pavement and rigid pavement (Nahak et al., 2019).

In general, flexible pavement uses an asphalt mixture as a binding material, which causes flexible pavement to have good flexibility and a layered structure. Therefore, in this pavement concept a double-layer elastic system (Multilayer Elastic System) is applied where materials used with higher quality are placed on the surface layer. Asphalt mixtures can also use natural aggregates which have a smooth surface but their binding properties are not very good (Tarigan, 2019). Aggregate characteristics are the main factor in determining the ability of road pavement to bear traffic loads and weather resistance (Faqih & Pramudiyanto, 2014). Road pavement construction that uses flexible pavement has several layer structures consisting of a surface layer (Surface Grade) which is spread on the base soil (Sub Grade), an upper foundation layer (Base course), and a lower foundation layer (Sub Base Grade) which each layer has a traffic load. The asphalt mixture in flexible pavement construction structures functions as a surface layer and uses granular material for the bottom layer (Arthono, 2022). Flexible pavement also has the function of distributing vehicle traffic loads which are distributed over each layer down to the subgrade (Maharani, 2018). Flexible pavement is used on roads with light to moderate traffic loads, for example on city roads, roads with utility infrastructure underneath, road shoulder pavement, or pavement that requires gradual construction (Sukirman, 2010). Road pavement construction can be divided into flexible pavement and rigid pavement (Nahak et al., 2019). Meanwhile, problems that usually occur in basic soil are deformation or differences in soil subsidence due to traffic loads, changes in water content, variations in soil type, and uneven compaction (Masriadi, 2018).

Flexible pavement has several mixtures, one of which is Thin Layer Asphalt Concrete (Lataston) which is known as Hot Rolled Sheet-Wearing Course (HRS-WC). Lataston is a type of surface layer that consists of two components, namely the wear layer (Lataston layer aus/HRS-WC) and the intermediate surface layer (Lataston layer between surfaces/HRS-Binder). The material used by Lataston is aggregate with a lame gradation dominated by sand and a high asphalt content, spread out and then compacted in a hot condition at a certain temperature (Badan Standardisasi Nasional Binamarga, 2007). To improve the quality of Lataston pavement, one method used is by adding materials and additives at the Asphalt Mixing Plant (AMP) which is called modified asphalt (Yusrizal, 2019). The part of flexible pavement construction that is located below the surface layer is the top foundation layer structure. The upper foundation layer functions to place the surface layer, support vehicle loads, and distribute vehicle loads to the structural layers below (Rumiati, 1993). Meanwhile, the lower foundation layer functions to distribute the load from vehicle wheels to the layer beneath it or to the subgrade layer (Afriansyah, 2023). The asphalt mixture in flexible pavement construction structures functions as a surface layer and uses granular material for the bottom layer (Arthono, 2022). The asbuton aggregate mixture layer has a minimum thickness of 40 mm with the largest size of aggregate grains being 19 mm (Asidin, 2022).

The addition of additional layers for continuous road improvements can cause asphalt and materials to decrease, therefore it is necessary to reprocess old pavement materials that are no longer used by adding filler, mixtures and new asphalt so that they meet construction requirements. This method of reprocessing unused asphalt (asphalt waste) is also called the recycling method. Sustainable reprocessing of asphalt waste can contribute to the creation of environmentally friendly construction services. Asphalt pavement waste can be reused as a very useful resource. The asphalt recycling process can be carried out using two methods, namely processing at the mixing site (In Plant) and processing directly in the field or (In Place). Processing at the mixing plant is the result of raking used asphalt which is taken to the mixing plant so that its properties can be improved, thickness adjusted, and the type of road recycling selected for use. Meanwhile, processing in the field is the process of raking, compacting and forming directly on the spot (Latjemma, 2022).

In making the HRS-WC mixture, aggregate is a very important part. Aggregates are divided into two categories, namely natural aggregates and artificial aggregates. Over time, the availability of natural aggregates has decreased due to increasing infrastructure development in Indonesia, as a result, natural materials that are used continuously can damage the environment. Therefore, an alternative is needed as a substitute for natural aggregate by utilizing residual waste from the stone crushing industrial process (Mahbubi, 2019). Stone ash is a type of fine aggregate that successfully passes through a sieve with a diameter of 4.75 mm and remains on a sieve with a size of 0.075 mm, so that stone ash can be used as a building construction mixture. Stone ash can be used as a filler to replace sand in asphalt mixtures (Handayani, 2019). Inspection of asphalt materials is carried out to ensure that one of the stability factors for pavement construction is met, as well as other aspects related to implementation in the field (Nugroho, 2019). Reclaimed Asphalt Pavement (RAP) itself was historically caused by the petroleum crisis in the 1970s and the increase in material prices (Frank et al., 2016). Due to the increasing price of materials for road pavement and awareness of damage to the environment, researchers have encouraged researchers to find pavement construction technologies that are more environmentally friendly and economical in terms of costs (Rathore et al., 2019).

The main objective of this research is to find the benefits of asphalt recycling by adding crushed stone ash as a Lataston mixture for flexible pavement. This data is very useful in saving flexible pavement construction costs, helps reduce the environmental impact of road construction, improves the quality of flexible pavement by incorporating recycled asphalt and rock ash in Lataston mixes, and contributes to improving road construction technology and practices, which can benefit the construction industry and Society.

METHODS

This research uses experimental and qualitative methods. Asphalt waste was substituted with new 60/70 penetration asphalt as a rejuvenating agent and filler was added using crushed stone ash. The object of this research is flexible pavement for Thin Layer Asphalt Concrete (LATASTON) mixtures. The planned mixture of new asphalt and recycled asphalt is with percentage variations of 2%, 2.5%, 3% and 3.5%. Meanwhile, the planned crushed stone ash content as filler is 3%, 5% and 7%. This research is expected to optimize asphalt waste and crushed stone ash waste for reprocessing and increase the stability of the Lataston mixture.

To analyze the results of Marshall testing, researchers used qualitative methods. Marshall testing aims to obtain stability values against static melting of recycled hot asphalt mixtures. The addition of new asphalt to asphalt waste functions as a rejuvenating agent, and the addition of crushed stone ash aims to ensure that the recycled hot asphalt mixture meets predetermined standard specifications. The results of the marshall test are expected to meet the requirements for thin layer asphalt concrete (Lataston) flexible pavement. The results of this research refer to the Specifications of the National Highways Standardization Agency (2007) concerning Guidelines for the Implementation of Hot Mixed Asphalt Layers.

The research location was carried out at the Road Construction Laboratory, Department of Civil Engineering and Planning Education, Faculty of Engineering, Yogyakarta State University. This test is carried out in stages starting from asphalt penetration testing and marshall testing. This testing was carried out from June 2023-September 2023. Testing was carried out in accordance with K3 standards to obtain the expected results.

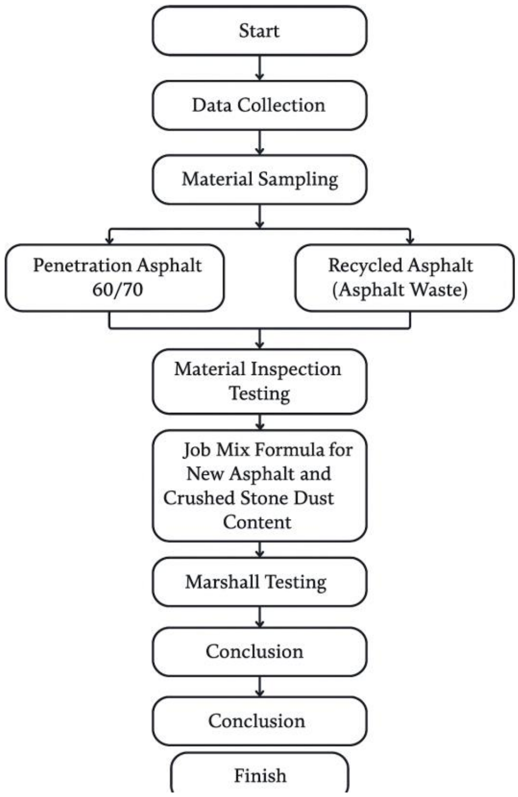

Figure 1. Flow Chart Research

The research was carried out by utilizing asphalt waste (asphalt recycling) obtained from road dredging on Jl. Wates, KM 12, Sedayu, Sleman, Yogyakarta. The results of dredging unused asphalt are then processed at the Road Construction Laboratory, Department of Civil Engineering and Planning Education, Faculty of Engineering, Yogyakarta State University. The used asphalt is then broken into smaller chunks to make the mixing process easier with new asphalt and crushed stone ash as a rejuvenator and filler for the Lataston pavement mixture. The used asphalt processing process used has limitations, where the aggregate in the used asphalt cannot be filtered to separate the aggregate and old asphalt attached to the pavement mixture.

Figure 2. Asphalt Waste from Dredging

FINDINGS

In this study, used asphalt (recycled asphalt) was used as a result of dredging the old pavement on Jl. Wates, KM 12, Sedayu, Sleman, Yogyakarta, as a research object to reprocess used asphalt that is no longer used so that it can be reused for flexible thin layer asphalt concrete (Lataston) pavement.

A. Asphalt Inspection Test Results

The quality of the ingredients in the asphalt concrete mixture can be determined by testing asphalt penetration, softening point, flash point, ductility, viscosity and specific gravity. The aim of the asphalt test is to indicate the asphalt's ability to withstand loads and temperature changes, as well as predicting the long-term performance of the road or asphalt surface. The results of the asphalt inspection test can be seen in Table 1.

Table 1. Results of Asphalt Inspection Testing

Test Type	Spec	Results	Requirements
Penetration, 25˚C; 100 gr; 5 seconds; 0.1mm	60-79	64,77 mm	OK
Softening point,˚C	48-58	51. 5˚C	OK
Flash point,˚C	Min 200	306˚C	OK
Ductility 25˚C, cm	Min 100	150 cm+	OK
Specific gravity	Min 1	1.044 gr/cc	OK

From the results of the material inspection tests above, it shows that the asphalt used meets the standard requirements set out in the Hot Mix Asphalt Coating Implementation Guide.

B. Marshall Test With the Addition of New Asphalt

In this Marshall test, new asphalt was added to the recycled asphalt mixture. Marshall testing for the addition of new asphalt to recycled asphalt is limited to the parameters Stability, Density, flow and Marshall Qountient. Based on the results of Marshall testing to determine the optimum asphalt content as a rejuvenating agent in recycled asphalt, the following results were obtained from the planned parameters

1) Stability

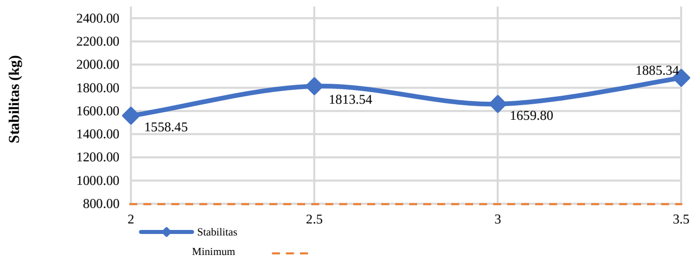

Figure 3. Stability Value Graph

Table 2. Stability Values from Marshall Testing

Asphalt Content (%)	**Stability (kg)**
2	1558.45
2	1558.45
2.5	1813.54
3	1659.80
3.5	1885.34

From Figure 3 and Table 2, the stability values from the marshall test results in this study have met the standard specifications required in the Hot Mix Asphalt Layer Implementation Guide (2007), for Lataston hot mix asphalt, namely a minimum of 800 kg.

2) Density

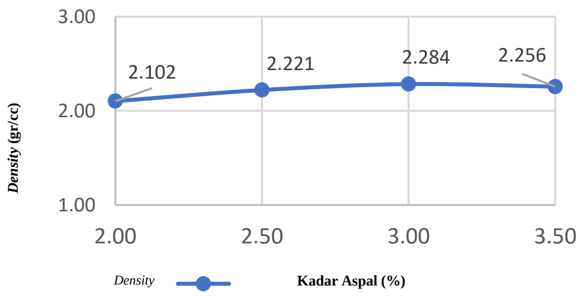

Figure 4. Density Value Graph

Table 3. Density Values from Marshall Testing

Asphalt Content (%)	**Density (gr/cc)**
2	2.102
2.5	2.221
3	2.284
3.5	2.256

From Figure 4 and Table 3 it can be seen that the density value from the Marshall test results in this study continues to increase up to an asphalt content of 3%, and slightly decreases at an asphalt content of 3.5%. Asphalt plays a very important role as a binding agent which causes the mixture to become denser.

3) Flow

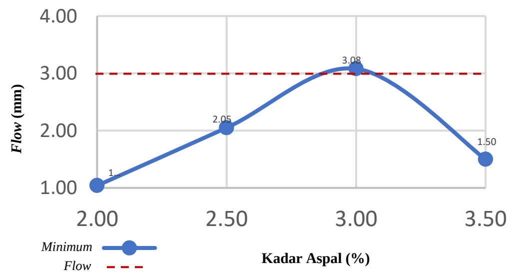

Figure 5. Flow Value Graph

Table 4. Density Flow from Marshall Testing

Asphalt Content (%)	**Flow (mm)**
2	1.04
2.5	2.05
3	3.08
3.5	1.50

From Figure 5 and Table 4, at an asphalt content of 3%, the flow value meets the standard specifications required in the Hot Mix Asphalt Layer Implementation Guide (2007) for Lataston hot asphalt mixes, namely a minimum of 3 (mm).

4) Marshall Qoutjent

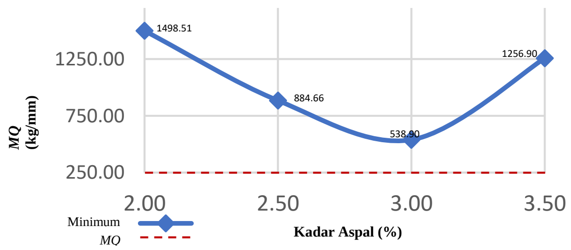

Figure 6. Marshall Qountient Value Graph

Table 5. MQ Values from Marshall Testing

Asphalt Content (%)	*Marshall Quontient* (kg/mm)
2	1498.51
2.5	884.66
3	538.90
3.5	1256.90

Figure 6 and Table 5 show that the marshall quotient quality in this study is in accordance with the requirements described in the Hot Mix Asphalt Layer Implementation Guide (2007) for Lataston hot mix asphalt, namely a minimum of 250 (kg/mm).

The best Optimum Asphalt Content (KAO) value is 3% asphalt content because it meets the Marshall criteria for Stability, Density, Flow and Marshall Qoutient. After obtaining KAO from the new asphalt content, testing of the asphalt trial mix will be continued with the addition of crushed stone ash as a filler. KAO from marshall testing with the addition of new asphalt to recycled asphalt can be seen in Figure 7 below:

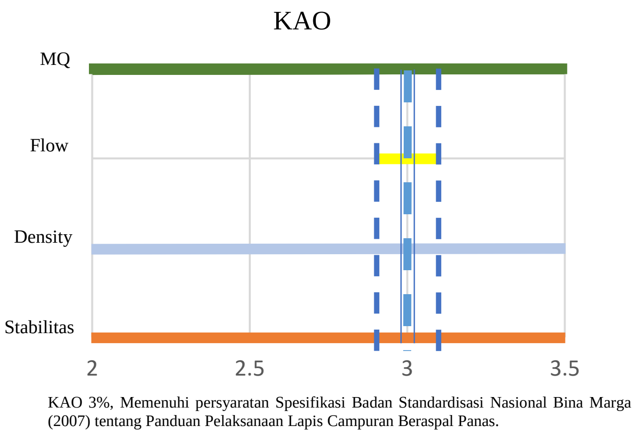

Figure 7. KAO Chart for New Asphalt Mixtures

C. Marshall Test with Addition of Crushed Stone Ash

In this research, crushed stone ash was also added which functions as a filler to fill empty cavities so that it can increase the flexibility and durability of the pavement. Testing was carried out using the Marshall method, Marshall parameters were limited to Stability, Density, Flow and Marshall Qoutient. Mixing recycled asphalt is carried out by adding 3% new asphalt and crushed stone ash to create a mix design.

1) Stability

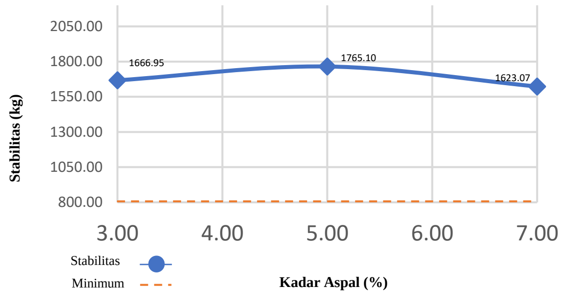

Figure 8. Stability Value Graph

Table 6. Stability Values from Marshall Testing

Asphalt Content (%)	Stability (kg)
3	1666.95
5	1765.10
7	1623.07

From Figure 8 and Table 6, the highest stability value is at a crushed stone ash content of 5% and decreases at a level of 7%. The stability value is in accordance with what is required in the Hot Mix Asphalt Layer Implementation Guide (2007) for Lataston hot asphalt mix, namely a minimum of 800 kg.

2) Density

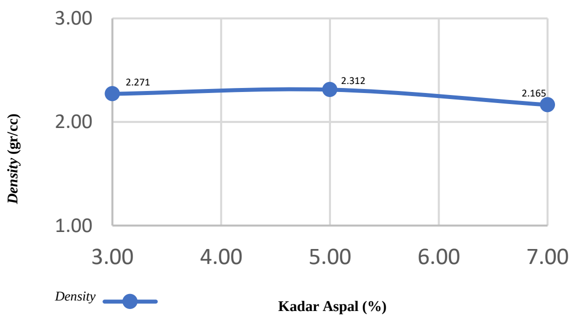

Figure 9. Density Value Graph

Table 7. Density Values from Marshall Testing

Asphalt Content (%)	Density (kg)
3	2.27
5	2.31
7	2.17

From Figure 9 and Table 7 it can be seen that the density value increased at a crushed stone ash asphalt content of 5% and fell again to the lowest value at a crushed stone ash content of 7%. The density value meets the standard specifications required in the Hot Mix Asphalt Layer Implementation Guide (2007) for Lataston hot mix asphalt

3) Flow

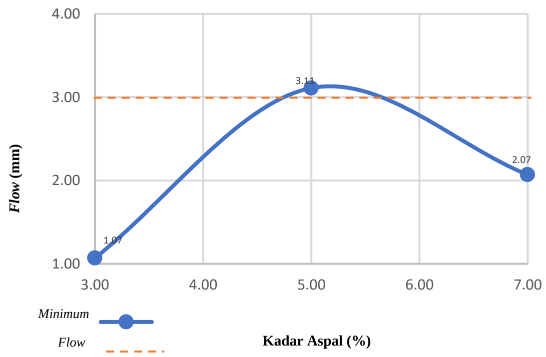

Figure 10. Flow Value Graph

Table 8. Flow Values from Marshall Testing

Asphalt Content (%)	Flow (mm)
3	1.07
5	3.11
7	2.07

From Figure 10 and Table 8, the flow value in the marshall test with the addition of crushed stone ash obtained the best value at a crushed stone ash content of 5%, and meets the standard specifications required in the Hot Mix Asphalt Layer Implementation Guide (2007) for Lataston hot asphalt mixes, namely minimum 3.0 mm.

4) Marshall Qoutjent

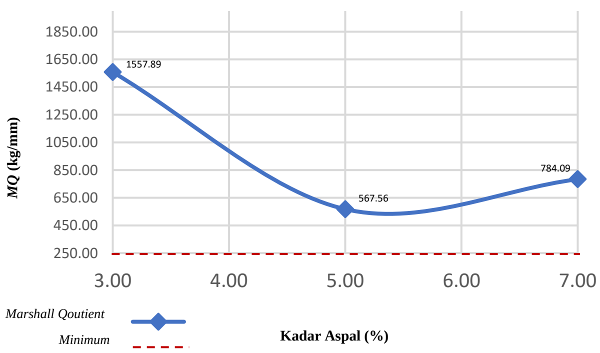

Figure 11. Marshall Qountjent Value Graph

Table 9. MQ Values from Marshall Testing

Asphalt Content (%)	*Marshall Quontient* (kg/mm)
3	1557.89
5	567.5
7	784.09

From Figure 11 and Table 9, the highest marshall qoutient value is at a crushed stone ash content of 3% and the lowest is at a crushed stone ash content of 5%. The marshall qoutient value in this study is in accordance with the specifications required in the Hot Mix Asphalt Layer Implementation Guide (2007) for Lataston hot mix asphalt, namely a minimum of 250 (kg/mm).

From the Marshall test results on the addition of new asphalt with a content of 3% and the addition of crushed stone ash to recycled asphalt, the Optimum Asphalt Content value for crushed stone ash was obtained at a crushed stone ash content of 5%. Marshall test results meet the Hot Mix Asphalt Layer Implementation Guide Specifications (2007) for Lataston hot asphalt mixes. KAO values and examination of Marshall test results on the addition of 3% new asphalt with crushed stone ash can be seen in Figure 12 below:

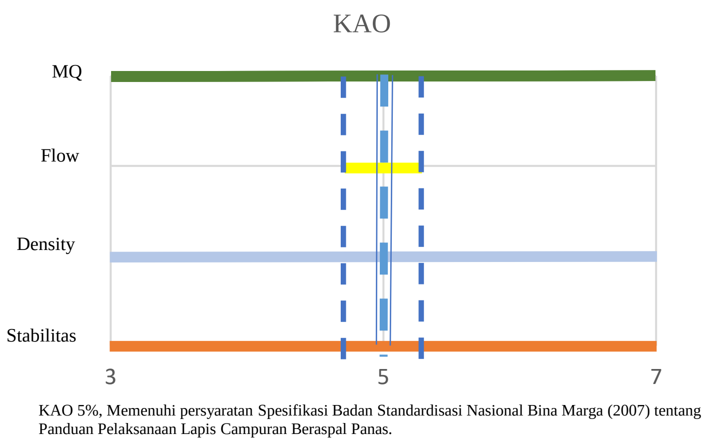

Figure 12. KAO Chart for Crushed Stone Ash Mixture

REFERENCES

Afriansyah, Y. (2023). Pelaksanaan Pekerjaan Pembangunan Jalan Dengan Base Course dan Subbase Course Untuk Mempertahankan Umur Rencana Jalan. Jurnal Archipelago, 1(2), 61-67.

Al Mahbubi, M. I. R. Z. A. (2019). Studi Penggunaan Agregat Buatan Berbahan Dasar *Fly Ash* Pada Agregat Kasar Terhadap Perkerasan Lentur Untuk Pengurangan Penggunaan Agregat Alam. *Institut Teknologi Sepuluh Nopember*

Arthono, A., & Permana, V. A. (2022). Perencanaan Perkerasan Lentur Jalan Raya Menggunakan Metode Analisa Komponen SNI 1732-1989-F Ruas Jalan Raya Mulya Sari Kecamatan

Pamanukan Sampai Kecamatan Binong Kabupaten Subang Propinsi Jawa Barat. Jurnal Komposit: Jurnal Ilmu-ilmu Teknik Sipil, 6(1), 41-51.

Asidin, A. (2022). Pengaruh Suhu Pada Penghamparan Lasbutag Campur Dingin Hampar Panas Menggunakan Lawele Granular Asphalt (LGA) Dan Modifier AC/Solar Terhadap Karakteristik Marshall. Jurnal Media Inovasi Teknik Sipil UNIDAYAN, 11(1), 58-71.

Badan Standardisasi Nasional Binamarga. (2007). Pedoman Pelaksanaan Lapis Campuran Beraspal Panas*: Vol. SNI 03-179* (p. 51). Menteri Pekerjaan Umum Republik Indonesia.

Faqih Ma'arif & Pramudiyanto. (2014). Uji Kinerja Marshall Agregat Bantak Merapi Dengan Menggunakan Serat Polypropylene. Inersia: lnformasi dan Ekspose Hasil Riset Teknik Sipil dan Arsitektur, 10(1).

Frank, R., Zaumanis, M., & Mallick, R. B. (2016). 100% Hot Mix Asphalt Recycling: Challenges and Benefits. Transportation Research Procedia, 14(April), 3493–3502.

Handayani, F. (2019). Manfaat Limbah Abu Batu Sebagai Tambahan Material Bahan Bangunan. S2Tekniksipil. Ulm. Ac. Id, 59-68

Maharani, A., & Wasono, S. B. (2018). Perbandingan Perkerasan Kaku Dan Perkerasan Lentur (Studi Kasus Ruas Jalan Raya Pantai Prigi-Popoh Kab. Tulungagung). Ge-STRAM J. Perenc. dan Rekayasa Sipil, 1(2), 89-94.

Masriadi, I. (2018). Analisa Perkerasan Lentur Terhadap Lapisan Pondasi Bawah. 77.

Nugroho, M. S. (2019). Karakteristik Marshall Quotient Pada Hot Mix Asphalt Menggunakan Agregat Alam Sungai Opak. INERSIA lnformasi dan Ekspose Hasil Riset Teknik Sipil dan Arsitektur, 15(2), 84-91.

Latjemma, S. (2022). Studi Analisis Pemamfaatan Hasil Pengupasan Aspal untuk Daur Ulang Campuran HRS-WC. *Jurnal Multidisiplin Madani*, *2*(10), 3678-3687.

Tarigan, G. (2019). Pengaruh Penggunaan Agregat Alam Pada Campuran Aspal Beton Terhadap Marshall Properties. In Seminar Nasional Teknik (SEMNASTEK) UISU (Vol. 2, No. 1, pp. 170-173).

Nahak, P. R., P, Y. C. S., & Winarto, S. (2019). Studi Perencanaan Tebal Perkerasan Konstruksi Jalan Raya Pada Ruas Jalan Umasukaer Di Kabupaten Malaka. *Jurmateks*, *2*, 11.

Rathore, M., Zaumanis, M., & Haritonovs, V. (2019). Asphalt Recycling Technologies: A Review on Limitations and Benefits. IOP Conference Series: Materials Science and Engineering, 660(1).

Rumiati, R. (2016). Tinjauan Struktur Perkerasan Jalan Trans Sulawesi Segmen Mohungo (Pada Ruas Jalan Sta 0.00–Sta 0.600). RADIAL: Jurnal Peradaban Sains, Rekayasa dan Teknologi, 4(2), 171-180.

Sukirman, S. (2010). Perencanaan Tebal Struktur Perkerasan Lentur. In Insitut Teknologi Nasional, Bandung (Vol. 53, Issue 9).

Yusrizal, Y. (2019). Analisis Karakteristik *Marshall* Campuran *Hot Rolled Sheet Wearing Course* (*HRS-WC*) Menggunakan BahanTambah Plastik Bekas Jenis *Polyethyleene Terephthalate*

(PET). *Prosiding Simposium* Forum Studi Transportasi Antar Perguruan Tinggi, l (November), 1–10.

JACEP

Journal of Applied Civil Engineering and Practices

Online (e-ISSN): e-ISSN XXXX-XXXX || **Printed (p-ISSN)**: p-ISSN XXXX-XXXX
2025, Volume 1, No 1, pp.27-37

Analysis Of Concrete Structure Calculation Methods Based on SNI 2847-2002 And SNI 2847-2023 using Etabs 21.2.0

Pradyta Galuh Oktafiani [a*], Satria Harta Winata[a], Chandra Nur Hanifah[a], Akhyar Arista Widya[a], Risang Sakha Purwandhato[a], Theyo Yuda Pratama[a], Hanif Lucky Syaifudin[a]

[a] Universitas Negeri Yogyakarta, Department of Civil Engineering, Faculty of Vocational, Indonesia

*Corresponding Author: pradytagaluh@uny.ac.id

To cite this article:
Oktafiani, et.al (2025). Alanysis of concrete structure calculation methods based on SNI 2847-2002 and SNI 2847-2023 unsing ETABS 21.2.0 *Journal of Applied Civil Engineering and Practices*, 1(1), Pp 27-37. doi: xx.xxxx/xxxxxx.xxxx.xxxxxx

To link to this article:
http://doi.org/10.22xx/xxxxxx.2023.xxxxxx

Journal of Applied Civil Engineering and Practice by Department Bachelor of Applied Science in Civil Engineering, Faculty of Vocational, Universitas Negeri Yogyakarta.

2025, Volume 1, No 1, pp.27-37, e-ISSN XXXX-XXXX

JACEP

Journal of Applied Civil Engieering and Practice

Journal homepage: https://journal.uny.ac.id/publications/jacep/index

Research paper

Analysis of Concrete Structure Calculation Methods Based on SNI 2847-2002 and SNI 2847-2023 using Etabs 21.2.0

Pradyta Galuh Oktafiani [a*], Satria Harta Winata[a], Chandra Nur Hanifah[a], Akhyar Arista Widya[a], Risang Sakha Purwandhato[a], Theyo Yuda Pratama[a], Hanif Lucky Syaifudin[a]

[a] Universitas Negeri Yogyakarta, Department of Civil Engineering, Faculty of Vocational, Indonesia
*Corresponding Author: pradytagaluh@uny.ac.id

ARTICLE INFO

Article History:
Received: March 07 2025
Accepted: May 20 2025
Published: May 20 2025

Keywords:
Design, safety, structural concrete

How To Cite:
Oktafiani, et.al (2025). Alanysis of concrete structure calculation methods based on SNI 2847-2002 and SNI 2847-2023 unsing ETABS 21.2.0 *Journal of Applied Civil Engineering and Practices*, 1(1), Pp 1-13. doi: xx.xxxx/xxxxxx.xxxx.xxxxxx

ABSTRACT

Purpose: This study aims to analyze the impact of the regulatory change from SNI 2847-2002 to SNI 2847-2013 on structural concrete, particularly in terms of calculation methods and structural modeling. The update in standards was introduced to enhance concrete quality and align with scientific advancements in structural engineering.

Methods/Design: The research compares manual calculations based on SNI 2847-2002 with analysis conducted using Microsoft Excel in accordance with SNI 2847-2013. The focus is on the dimensions of reinforced concrete beams and the required Ace value (area of tensile reinforcement), which significantly influences structural performance.

Findings: A significant difference in the Ace values was observed between the two standards. This discrepancy arises due to variations in the effective depth (*d*) and the sliding moment formula applied in each version of the standard. These differences directly affect various structural aspects, including flexural strength, stiffness, crack control, and beam deflection.

Practical implication: The transition from SNI 2847-2002 to SNI 2847-2013 has implications not only for technical calculations but also for structural design and safety. Structural engineers must understand and adapt to these changes to ensure their designs comply with updated standards and meet enhanced safety requirements.

INTRODUCTION

Concrete is a mixture of Portland or hydraulic cement with fine aggregate, coarse aggregate, and water, sometimes with admixtures (Alfatari et al., 2021 ; Gracia and Gonzalez

2018). Reinforcement is used in concrete to resist tensile forces, as concrete is strong against compressive forces but weak against tensile forces (Nawy & Edward, 1998). Reinforced concrete contains a minimum-required cylinder and design so that both materials work together to withstand the style (Mulyono, 2004). In Indonesia, reinforced concrete planning standards refer to SNI 2847:2013. Reinforced concrete beams are essential in building construction, especially in multi-storey residential buildings. Reinforced concrete combines concrete (strong in resisting compressive forces) and reinforcing steel (strong in resisting tensile forces). This combination creates a composite material that can withstand various loads and forces in building structures. Reinforced concrete is used in various structural elements such as beams, columns, slabs, and foundations, where reinforced concrete beams, in particular, resist bending and shear loads and transfer loads from floor slabs to columns or load-bearing walls. In concrete planning, Indonesia has regulations and standards that regulate its planning, namely the Indonesian National Standard or SNI.

The Indonesian National Standard (SNI) is a set of regulations established by the National Standardization Agency (BSN) and is legally binding at the national level. These standards are designed to protect and ensure the uniformity of various products, including buildings. In the context of building construction, standardization encompasses all aspects—from initial planning and structural strength calculations to construction practices, testing, and long-term maintenance. On December 17, 2019, BSN officially enacted a revised standard for structural concrete, namely SNI 2847:2013, which superseded the previous SNI 2847:2002 titled *Structural Concrete Requirements for Buildings*. This update was introduced with the intention of enhancing the quality and reliability of concrete structures, while also aligning national practices with ongoing scientific and engineering developments in structural concrete design.

The shift from the 2002 to the 2013 version of the standard holds significant implications, especially in the context of structural safety and serviceability. Because building feasibility must consider both strength and safety criteria, any ongoing or previously planned concrete structure designs based on the older standard may need to be reviewed and revised. This change does not occur in isolation—other related SNI regulations have also been updated. For instance, updates in earthquake-resistant building standards have influenced the response spectrum, leading to increased shear forces in structural elements (Aditya et al., 2021; Sucipto & Sutjipto, 2022). Given these developments, there is a pressing need to evaluate how the transition from SNI 2847:2002 to SNI 2847:2013 affects structural concrete, particularly in terms of analytical calculations and structural modelling practices. This research aims to identify and analyze the key differences between these two standards and assess their practical impact on reinforced concrete behavior, performance, and design parameters.

The transition of structural design codes in Indonesia reflects a broader trend toward harmonizing national standards with international best practices and updated scientific understanding. SNI 2847, which governs the requirements for structural concrete design, is largely adapted from the American Concrete Institute (ACI) 318 standards. The update from SNI

2847:2002 to SNI 2847:2013 corresponds closely with changes seen in ACI 318-08, incorporating more rigorous design procedures and enhanced safety considerations.

Previous studies have noted that one of the most significant changes in SNI 2847:2013 lies in the reformulation of load and resistance factors, revisions in shear and moment calculations, and adjustments to reinforcement detailing. These changes aim to improve structural performance under both static and dynamic loads (ACI Committee 318, 2008). For example, the sliding moment equation and parameters such as the effective depth (d) and area of tensile reinforcement (Ace) were revised, resulting in noticeable differences in structural dimensions and reinforcement requirements (Aditya et al., 2021). In the Indonesian context, Sucipto & Sutjipto (2022) emphasized that the updated concrete standard affects not only the strength design but also building behavior under seismic conditions. When integrated with revised seismic codes (e.g., SNI 1726:2019), the combined effect can result in increased base shear forces and higher structural demands, especially in earthquake-prone areas. These changes necessitate more conservative and robust design strategies.

Moreover, comparative analyses between SNI 2847:2002 and SNI 2847:2013 conducted in various structural modeling software, such as ETABS or SAP2000, show disparities in beam deflection, crack width control, and overall stiffness, all attributed to different assumptions and design methodologies embedded in the two versions (Yulianto & Arifianto, 2020). Such findings underscore the importance of understanding the structural implications of code changes beyond mere numerical differences in reinforcement. Despite growing awareness of these differences, there is still limited empirical research focusing specifically on how manual calculations and digital tools reflect the transition between these two SNIs. Most existing literature focuses either on isolated parameters or on software-based simulations, with few studies providing a comprehensive comparison that integrates manual calculation methods with modeling outcomes based on both standards. This gap highlights the need for research that systematically examines the practical implications of the standard update, especially from a design and engineering decision-making perspective. By exploring these changes in a detailed, comparative manner, this study contributes to a better understanding of how regulatory evolution shapes real-world engineering practices.

METHODS

1. Case Study Details

The case study refers to the research of (Septiropa, 2009) which discusses the optimization of reinforced concrete beam dimensions in simple multi-storey houses based on SNI 2847-2002. Furthermore, from the same case study as the research and calculations of Septioropa, 2009, we re-analyzed by considering aspects of SNI changes to the latest regulations, namely SNI 2847-2013. This update includes significant changes in calculation methods and technical requirements, which aim to improve the quality and safety of building structures. This case study aims to optimize the dimensions of reinforced concrete beams in a simple multi-storey house using the latest standard, SNI 2847:2013. The main focus is to design beams that meet structural strength and stability requirements and are efficient in material use, resulting in an economical design without compromising safety aspects.

2. Building Beam Planning Data

The building beams are planned by calculating a residential house with type 36, 2 floors, a land area of 80 m2, two bedrooms, a kitchen, a bathroom, and a living room that integrates with the family room. Figure 1 illustrates the house plan, and beam planning data can be seen in Table 1.

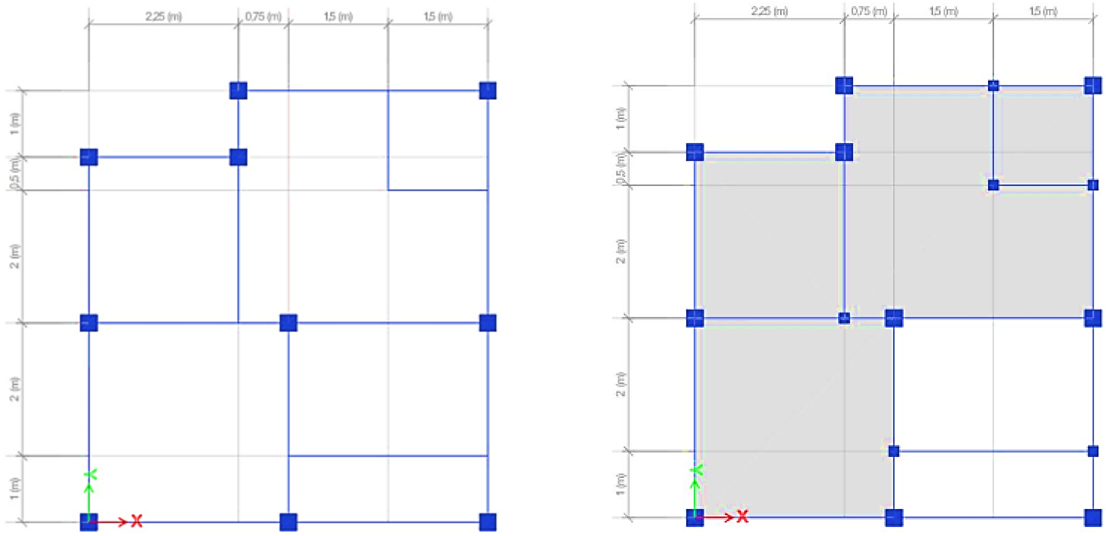

(a) (b)

Figure 1 House Floor Plan (Septiropa, 2009) (a) Fist Floor, (b) Second Floor

Table 1 Building beam planning data

No	Data	Vol	Unit
1	Beam thickness (h)	350	Mm
2	Beam width (b)	250	mm
3	Fc’	22.5	MPa
4	Fy	240	MPa
5	Beam span length (L)	3	m
6	Beam width (b)	1.5	m
7	Dead load (qd)	4.07	kN/m^2
8	Live load (ql)	1.25	kN/m^2
9	Beam load	1.38	kN/m^2

3. Structural Calculations

In reinforced concrete planning/calculation, two conditions must be met, namely:

a. The design moment Md must ≥ necessary momen Mu.
b. Concrete compressive strain ε'c must ≤ limit strain ε'cu (0,003).

Calculation of beam longitudinal reinforcement, using the equation:

$$K = \frac{Mn}{bd\text{^}2} \text{ or } K = \frac{Mu}{\phi.\text{b.d}\text{^}2} \quad (1)$$

$$a = (1 - \sqrt{1 - \frac{2k}{-,85\, f\prime c}}).\, D \quad (2)$$

$$As = \frac{0{,}85\, f'.a.b}{fy} \quad (3)$$

The calculation design moment Md is carried out as follows:

a. The equivalent square concrete compressive stress beam height a is:

$$a = \frac{As\, fy}{0.85.f\prime c.b} \quad (4)$$

b. Actual moment Mn with equation:

$$Mn = Cc.\ (d-\frac{a}{2}) \text{ or } Mn = Ts.\ (d-\frac{a}{2}) \quad (5)$$

Then the design moment Md = θ. Mn with θ = 0,9

The equation calculates the concrete compressive strain:

$$\mathcal{E}'c = \frac{a}{\beta 1.d}\, \mathcal{E}'y \quad (6)$$

With the condition that it must be ≤ 0,003

4. Structural Modelling

The structural analysis uses two methods: manual calculation of beam design using Microsoft Office Excel and structural design modelling using the ETABS 21.2.0 application. Finite element-based computer calculations for various loading combinations, including dead and live loads, are combined with 3D structural modelling. The input of ETABS structural planning data is based on the Indonesian Loading Regulations for Buildings 1983.

FINDINGS

1. Research Data Load Calculation

Dead load is the weight of all fixed parts of a building, including all ancillary elements, finishes, machines, and fixed equipment that are integral to the building. The dead load on this multi-storey house planning is:

a. Floor 0,24 kN/m^2 = 0,24 kN/m^2 a) Weight of Floor Covering 0.24 kN/m^2 = 0.24 kN/m^2
b. Weight of Speci Mix 0.21 kN/m^2 = 0.21 kN/m^2
c. Weight of backfill Sand 16 kN/m^3 x 0.05 m = 0.8 kN/m^2
d. Self Weight of Concrete Plate 24 kN/m^3 x 0.11 m = 2.64 kN/m^2
e. Ceiling Hanging Weight 0.07 kN/m^2 = 0.07 kN/m^2
f. Weight of Frame and Ceiling 0.11 kN/m^2 = 0.11 kN/m^2
g. Total = 4.07 kN/m^2
h. Live load for simple Residential Building Use Load = 125 kN/m^2 = 1.25 kN/m^2

2. Data Analysis And Calculation Regarding SNI 2847-2013

Calculations carried out using the formula and reference SNI 2847-2013 obtained the following values:

Table 2 Excel Calculation Results

Ultimate uniform load (qu)	8,54 kN/m2
Necessary moment in the beam (Mu)	96,067,500 Nmm
Design moment in the beam (Md)	24,930,000 Nmm
Plan moment in the beam (Mr)	18,165,247.85 Nmm
Bending moment (k)	0.44 Mpa
Quantity of Reinforcement (n)	3D12 Where made into 4D12 with 2 compressive reinforcement and 2 tensile reinforcement
Reinforcement ratio	0.0062 with qualified > ρmin which is 0.005 and < ρmax which is 0.04.

Table 3 Beam cross-section details

Type	Pedestals
Beam 25/35	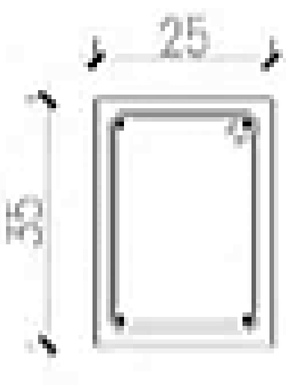
Concreate ducking	40 mm
Tensile reinforcement and compressive reinforcement	2Ø12
Begel	-

In addition to performing the analysis by calculation, further analysis was carried out using ETAPS with the load combination used 1.2D +1.2 SDL + 1.6L. Planning is carried out on the house's structure according to the plan, and the results can be seen in Figure 3. The moments usually wanted to be obtained on the beam are the pedestal area ¼ span and the field area ½ span. Mu = 6.2 kN / m in the middle of the span, and the value of Mu = -7.8 kN / m at the end of the span. Table 3 describes the beam element loads in ETAPS 21.2.0 calculations.

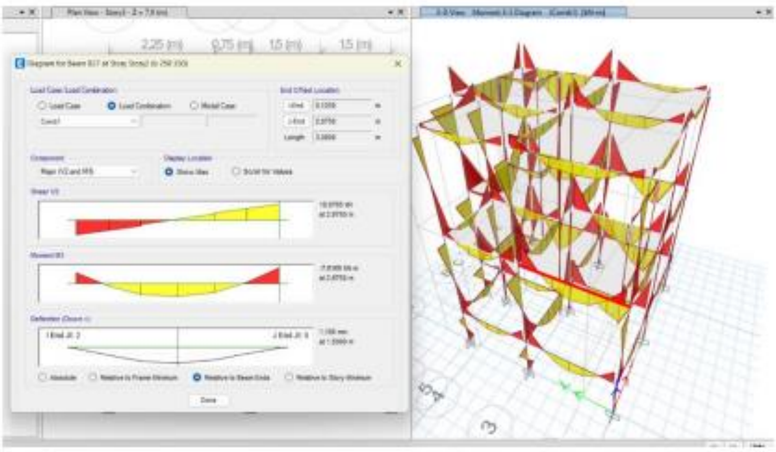

Figure 2 Result ETAPS

The figure shows the results of structural analysis using ETABS software, where moment, shear and deflection diagrams of one of the beams on the second floor of a multi-storey building structure are shown. Based on the displayed internal force diagram, it can be seen that the beam experiences the maximum moment at mid-span as well as the maximum shear force near the pedestal, which is indicated by the red-colored area as an indication of extreme values. The maximum deflection of the beam was recorded at 1,306 mm, which is still within the service tolerance limit of the structure. The analysis utilizes a combination of loads, which reflects the actual condition of the structure under the simultaneous influence of dead, live, and lateral loads. These results provide important information for the reinforcement planning process and evaluation of the structure's performance against safety and comfort criteria in accordance with applicable planning standards.

Element Forces - Beams											
Story	Beam	Output Case	Station	P	V2	V3	T	M2	M3	Element	Elem Station
Story2	B27	Comb1	0,125	0,121	-17,49	-0,026	1,0962	-0,017	-5,393	102-1	0,125
Story2	B27	Comb1	0,5625	0,121	-12,21	-0,026	1,0962	-0,006	1,1039	102-1	0,5625
Story2	B27	Comb1	1	0,121	-6,928	-0,026	1,0962	0,0052	5,2901	102-1	1
Story2	B27	Comb1	1	0,205	-5,023	0,0074	0,0637	0,0027	5,2221	102-2	0
Story2	B27	Comb1	1,5	0,205	1,0125	0,0074	0,0637	-0,001	6,2247	102-2	0,5
Story2	B27	Comb1	2	0,205	7,0481	0,0074	0,0637	-0,005	4,2096	102-2	1
Story2	B27	Comb1	2	0,233	8,4141	-0,017	-0,917	0,0004	4,1667	102-3	0
Story2	B27	Comb1	2,4375	0,233	13,695	-0,017	-0,917	0,0076	-0,67	102-3	0,4375
Story2	B27	Comb1	2,875	0,233	18,977	-0,017	-0,917	0,0149	-7,817	102-3	0,875

Figure 3 Result from ETABS

Based on the analysis that has been carried out using Microsoft Excel and ETAPS 21.2.0, there are some differences in the calculation results that have been obtained, among others, the load obtained by the beam, shear (strain), and moment on the beam with details shown in Table 4.

Table 4 differences in the calculation results using Excel and ETAPS

No	Differences	Excel	ETAPS 21.2.0
1	Load obtained by the beam	8.54 kN/m’	8.004 kN/m’
2	Shear	Not calculated	0
3	Moment in Beam	9.6075 kNm	4.9388 kNm

3. Analysis Of Differences Between SNI 2847-2002 And SNI 2847-2013

The results of the analysis show several differences in the formula between SNI 2847-2002 and SNI 2847-2013, as shown in Table 5.

Table 5 differences in the formula between SNI 2847-2002 and SNI 2847-2013 ([BSN] Badan Standarisasi Nasional, 2002, 2013)

INDICATORS	SNI 2847-2002	SNI 2847-2013
Bending Moment	$Mn = As.fy(d - \frac{a}{2})$ $a = \frac{As.fy}{0,85\ f'c.b}$	$Mn = As.fy(d - \frac{a}{2})$ $a = \frac{As.fy}{\beta 1\ f'c.b}$
Shear Capacity	Vn = Vc +Vs $Vc = 0,17\sqrt{f'cbwd}$ Vs is the contribution of shear reinforcement	Vn = Vc+ Vs $Vc = 0,17\sqrt{f'cbwd}$ Or $Vc = 0,29\sqrt{f'cbwd}$

		for condition without shear reinforcement
Crack Control	$wmax = \frac{2\sigma(dc + 0{,}5s)}{Es}$	$wmax = \frac{ptfs(dc + s/2)}{Es}$
Beam Deflection	$\Delta = \frac{5wL^4}{384EI}$	$\Delta = \frac{5wL^4}{384EIe}$
Reinforcement Minimum	$As \geq \frac{0{,}25\, f'c.b.d}{fy}$	$As \geq 0{,}0018.b.h$ Where b is the width of the beam and h is the total height of the beam

Table 5 shows that there are differences between SNI 2847-2002 and SNI 2847-2013 in terms of the calculation of reinforced concrete beams. The change in bending moment between the two standards shows the variation in concrete quality. Regarding shear capacity, SNI 2847-2013 increases flexibility and safety compared to SNI 2847-2002. Controlling the maximum crack width and minimum reinforcement requirements provides details to ensure that each beam has a minimum amount of reinforcement sufficient to cope with the base flexural load. This approach reduces the risk of failure and ensures the structure remains safe and stable under various load conditions.

In the calculation using SNI 2847-2002, the value of As needs to be 162.34 mm2. While the calculation results using SNI 2847-2013 obtained a value of As need of 382.932 mm2. There is a significant comparison with a difference of 220.592 mm2. This is due to the difference in the value of d (Longitudinal Beam Reinforcement). In the journal, the value of d is obtained at 281.5mm with the formula d = h - concrete blanket - ½ diameter of the central reinforcement rent. In Excel calculations, the value of d is obtained at 310 mm with the formula d = h -ds. In addition, the difference in the bending moment formula also affects the calculation of the required As. The As value used affects various aspects of structural performance, including flexural strength, stiffness, crack control, and beam deflection. Using too small or too large each has significant advantages and disadvantages for structural safety. The following are the effects of small and large As values on reinforced concrete beams:

A. As Value that is too Small
   1. Flexural Strength
      Insufficient steel reinforcement may cause the beam to be unable to resist the bending moment generated by the applied load. This situation can lead to flexural failure, where the concrete in the tensile section cracks and the steel reinforcement is insufficient to resist the stresses. In addition, flexural failure may occur earlier than planned (Wahiddin et al., 2022).
   2. Poor Crack Control

Insufficient reinforcement can lead to greater crack width in concrete. Excessive cracking can also reduce the beam's stiffness and the structure's overall performance (Noorhidana & Purwanto, 2011).

3. Excessive Deflection

   Lack of steel reinforcement can cause excessive deflection in the beam. Excessive deflection can compromise occupant comfort, mainly if the beam is used on a frequently passed or occupied floor (purnamasari, 2017).

B. As Value that is too Large

1. Inefficient Cost

   Excessive use of steel reinforcement increases material costs significantly. Increasing the amount of reinforcement can also increase the cost of the work, including installing and compacting the concrete around the reinforcement.

2. Construction Difficulties

   Too much reinforcement can make it difficult to place and compact concrete around the reinforcement, which can cause honeycombing and reduce concrete quality. Difficulties in reinforcement placement and concrete compaction can result in poor quality control, potentially reducing the long-term performance of the structure.

3. Increase in Self-load

   The addition of steel reinforcement also increases the dead load of the beam. While this may not be significant in some cases, in large structures or with other additional loads, the increase in dead load can affect the structure's overall design.

4. Over-Reinforced Section
5. Beams with too much reinforcement can become over-reinforced, where the steel reinforcement reaches yield stress after the concrete in the compressive section has collapsed (Apryanto & Hartopo, 2022).

SUMMARY

Based on the results and discussions that have been carried out, several conclusions can be drawn, including:

1. In the dimensional analysis of reinforced concrete beams, there is a significant difference between the necessary As value obtained through a manual calculation based on SNI 2847-2002 and analysis using Excel based on SNI 2847-2013. This difference is caused by variations in the value of d (Beam Longitudinal Reinforcement) and the bending moment formula used. The required As value affects various aspects of structural performance, including flexural strength, stiffness, crack control, and beam deflection.
2. Analysis using Microsoft Excel and ETAPS 21.2.0 showed differences in the beam's calculation of load, shear, and moment. Excel produced a beam load of 8.54 kN/m' and a moment of 9.6075 kNm, while ETAPS 21.2.0 showed a load of 8.004 kN/m', a strain of 0, and a moment of 4.9388 kNm.

REFERENCES

[BSN] Badan Standarisasi Nasional. (2002). *Standar Tata Cara Perhitungan Struktur Beton untuk Bangunan Gedung (SNI 03-2847-2002)*.

[BSN] Badan Standarisasi Nasional. (2013). *Persyaratan beton struktural untuk bangunan gedung, SNI 2847:2013*.

Aditya, R. A., Nurjaman, A., & Widodo, H. (2021). Analisis perubahan nilai gaya dalam elemen struktur akibat revisi SNI beton dan gempa pada gedung bertingkat. *Jurnal Karya Teknik Sipil*, *10*(1), 25–34. https://doi.org/10.1234/jkts.v10i1.2021

American Concrete Institute. (2008). *Building code requirements for structural concrete (ACI 318-08) and commentary*. American Concrete Institute.

Apryanto, T., & Hartopo, H. (2022). Kajian Hubungan Antara Dimensi Penampang, Mutu Baja Dan Mutu Beton Terhadap Nilai Daktilitas Beton Bertulang. *Teknika*, *17*(2), 127. https://doi.org/10.26623/teknika.v17i2.5423

García, R. A., & González, J. A. (2018). Optimal cement mixtures containing mineral admixtures under multiple and conflicting criteria. *Advances in Civil Engineering, 2018*, 1–13. https://doi.org/10.1155/2018/3780810

Mulyono, T. (2004). *Teknologi Beton*. Andi.

Nawy, & Edward, G. (1998). *Beton Bertulang Suatu Pendekatan Dasar*. Erlangga.

Noorhidana, V. A., & Purwanto, E. (2011). PENGARUH PELUBANGAN PADA BADAN BALOK BETON BERTULANG TERHADAP KAPASITAS BEBAN LENTUR. *Jurnal Rekayasa*, *15*(2).

Purnamasari, eka. (2017). ANALISA PERILAKU BALOK TINGGI DENGAN VARIASI PANJANG PERKUATAN GESER. *PROSIDING HASIL PENELITIAN DOSEN UNISKA*, 1–23.

Septiropa, Z. (2009). OPTIMASI DIMENSI BALOK BERTULANG PADA RUMAH BERTINGKAT SEDERHANA BERDASARKAN SNI -2847-2002 (SUBPROGRAM II PROGRAM PERENCANAAN TULANGAN BETON). *GAMMA*, *IV*(2), 153–160.

Sucipto, D., & Sutjipto, S. (2022). Pengaruh perubahan SNI 2847 terhadap kekuatan dan perilaku struktur bangunan tahan gempa. *Jurnal Teknik Struktur dan Konstruksi*, *8*(2), 45–55. https://doi.org/10.5678/jtsk.v8i2.2022

Wahiddin, Agus Sugiarto, & Joko Setiono. (2022). Pengaruh Dimensi Penampang Terhadap Rasio Desain Dan Lendutan Pada Inverted Beam. *Jurnal Teknik Ilmu Dan Aplikasi*, *3*(2), 129–133. https://doi.org/10.33795/jtia.v3i1.111

Yulianto, A., & Arifianto, H. (2020). Perbandingan hasil desain balok beton bertulang berdasarkan SNI 2847:2002 dan SNI 2847:2013 menggunakan perangkat lunak ETABS. *Jurnal Rekayasa Sipil dan Teknologi*, *6*(3), 112–121. https://doi.org/10.3333/jrst.v6i3.2020

JACEP

Journal of Applied Civil Engineering and Practices

Online (e-ISSN): e-ISSN XXXX -XXXX || **Printed (p-ISSN)**: p-ISSN XXXX-XXXX
2025, Volume 1, No 1, pp.38-50

Performance Evaluation of Low-Rise Steel Structures Using Pushover Analysis (Case Study Of Jeep Indonesia Brand Center Alam Sutera Showroom Building)

Zahran Maula Chandra Ar Razaq[a], Faqih Ma'arif[b*]

[a]Universitas Negeri Yogyakarta, Department of Civil Engineering, Faculty of Vocational, Indonesia
[a]Universitas Negeri Yogyakarta, Department of Civil Engineering and Planning Education, Faculty of Engineering, Indonesia

*Corresponding Author: faqih_maarif07@uny.ac.id

To cite this article:
Ar Razaq ZMC, Ma'arif F (2025). Performance Evaluation of Low-Rise Steel Structures Using Pushover Analysis (Case Study Of Jeep Indonesia Brand Center Alam Sutera Showroom Building). *Journal of Applied Civil Engineering and Practices*, 1(1), Pp 38-50. doi: xx.xxxx/xxxxxx.xxxx.xxxxxx

To link to this article:
http://doi.org/10.22xx/xxxxxx.2023.xxxxxx

Journal of Applied Civil Engineering and Practice by Department Bachelor of Applied Science in Civil Engineering, Faculty of Vocational, Universitas Negeri Yogyakarta.

2025, Volume 1, No 1, pp.38-50, e-ISSN XXXX-XXXX

Journal of Applied Nature and Construction

Journal homepage: https://journal.uny.ac.id/publications/jacep/index

Research paper

Performance Evaluation of Low-Rise Steel Structures Using Pushover Analysis (Case Study of Jeep Indonesia Brand Center Alam Sutera Showroom Building)

Zahran Maula Chandra Ar Razaq[a], **Faqih Ma'arif**[b*]

[a]Universitas Negeri Yogyakarta, Department of Civil Engineering, Faculty of Vocational, Indonesia
[a]Universitas Negeri Yogyakarta, Department of Civil Engineering and Planning Education, Faculty of Engineering, Indonesia
*Corresponding Author: faqih_maarif07@uny.ac.id

ARTICLE INFO

Article History:
Received: March 14 2025
Accepted: May 05 2025
Published: May 20 2025

Keywords:
ATC-40, Performance Point, Pushover Analysis, Structural Performance Level

How To Cite:
Ar Razaq ZMC, Ma'arif F (2025). Performance Evaluation of Low-Rise Steel Structures Using Pushover Analysis (Case Study Of Jeep Indonesia Brand Center Alam Sutera Showroom Building). *Journal of Applied Civil Engineering and Practices*, 1(1), Pp 38-50. doi: xx.xxxx/xxxxxx.xxxx.xxxxxx

ABSTRACT

Purpose: Indonesia is a country prone to earthquakes, and earthquakes can cause significant losses such as damage to infrastructure, buildings and loss of life. The objectives of this research are: (1) to determine the structural performance level of the Jeep Indonesia Brand Center Alam Sutera showroom building based on the ATC-40 method, (2) to determine the structural performance of the Jeep Indonesia Brand Center Alam Sutera showroom building based SNI 1726: 2019 regulations.
Methods/Design: The methods used in this research are: (1) 3D structural modeling using ETABS software, (2) calculate and determine the load on the structure based on SNI 1727: 2020, (3) perform earthquake load analysis to check the deviation between permit levels (Δ) according to SNI 1726: 2019 regulations, (4) perform pushover analysis using ETABS software to obtain performance points, (5) evaluate the structural performance level using the ATC-40 method from the calculation of the drift ratio obtained from the performance point results.
Findings: The results showed that: (1) based on the performance points obtained, the maximum total deviation value for x direction = 0.01011 and y direction = 0.00858. While the maximum inelastic deviation value for the x direction = 0.00811 and y direction = 0.01085.
Practical implication: This shows that the performance level of the Jeep Indonesia Brand Center (JIBC) Alam Sutera showroom building structure based on the ATC-40 method is Damage Control (DC), namely the building suffered minor damage due to the earthquake, but the damage can be repaired at an affordable cost and the risk of human casualties is very small, (2) the performance of the building structure still meets the requirements according to Table 20 of SNI 1726: 2019 which is indicated by the value of drift or deviation between floors that is not more than the deviation between permission levels (Δ).

INTRODUCTION

According to (Choerudin, 2008), Indonesia is a country that is very prone to earthquakes. This is because Indonesia is located in a meeting area between three large tectonic plates, namely the Indo-Australian, Eurasian and Pacific plates. Earthquakes in Indonesia often occur and cause significant losses such as damage to materials, infrastructure, buildings and fatalities. (Warsono & Budianto, 2019). This shows the need for structural performance evaluation and better earthquake prevention efforts. (Satria, 2022). Evaluation of the level of structural performance is a process carried out with the aim of determining the ability of a building to withstand earthquake loads and perform its functions properly during and after an earthquake. (Aldo & Pratama, 2019).

In addition, this evaluation aims to provide information about the condition of the structure and assist in making decisions about necessary repairs or renovations to ensure optimal performance in the long term. (Comartin, 1996). Evaluation of structural performance can be done by conducting earthquake load analysis using non-linear static analysis, namely pushover analysis. According to (Nuraga et al., 2021), Pushover analysis is one method in analyzing building structures with the aim of being able to determine the nature of the collapse of a building structure. Pushover analysis is carried out by giving the building structure a form of lateral load, then gradually increasing it so that it reaches a target displacement in the building. (Dewobroto, 2005). The primary purpose of a pushover analysis is to determine whether a building meets required performance specifications, such as safety and skill levels, and to provide information about structural weaknesses and strengths to assist in planning repairs or renovations. (Hakim, 2013). Pushover analysis is an important part of structural performance evaluation and is very useful in ensuring that buildings can function safely and effectively in earthquake situations. (Hakim et al., 2014).

According to (SNI 1726, 2019), regarding Earthquake Resistance Planning Procedures for Building and Non-building Structures, drift values (Δ) or the deviation between floors must meet the requirements and must not exceed the permitted deviation limit between levels (Δ) that has been determined. The deviation between floors is obtained by conducting static and dynamic earthquake load analysis. Based on (Ismaeil et al., 2015), The building must calculate its drift ratio value to obtain the building risk category calculated based on the performance point value obtained from the pushover analysis results. Based on the drift ratio value, the building is divided into four conditions, namely Immediate Occupancy, Damage Control, Life Safety, and Structural Stability. (Khouy et al., n.d.).

Figure 1. Jeep Indonesia Brand Center Alam Sutera Showroom Building

The Jeep Indonesia Brand Center (JIBC) showroom building is a three-story building with a steel structure located in Alam Sutera, South Tangerang, Banten. The Jeep Indonesia Brand Center Alam Sutera showroom building is a building that functions as a commercial building for Jeep vehicles and is used as an office on the second and third floors. In this building, it is necessary to carry out an earthquake load analysis and evaluate the structural performance level using the pushover analysis method with the help of ETABS software. (Scandura, 2009). The evaluation was carried out using pushover analysis to determine the performance of the building structure during an earthquake and to determine which areas are vulnerable to the structure. (Hutama, 2021).

METHODS/DESIGN

The object of the study is the Jeep Indonesia Brand Center (JIBC) showroom building located on Jl. Jalur Sutera Boulevard Kav. 30, Alam Sutera, South Tangerang, Banten. The Jeep Indonesia Brand Center building is a steel structure building with a height of three floors and a roof. The data used in this study are secondary data.

Table 1. Building Description

Biulding Name	Jeep Indonesia Brand Center
Vulding Function	Office and commercial buildings
Number of floor	3
Typical floor heght	4 m
Height from ground level	14.95 m

The research was conducted by conducting an analysis using non-linear static analysis, namely pushover analysis using ETABS software to obtain the level of building structure performance. The procedure used in this study uses the ATC-40 method and refers to the regulations (SNI 1726, 2019). This research was conducted by carrying out several stages as follows:

1. Collecting data on the structure of the Jeep Indonesia Brand Center showroom building. The data collected is in the form of shop drawings and construction management data used based on existing data.
2. Retrieval of spectrum response design data on the page https://rsa.ciptakarya.pu.go.id/
3. Three-dimensional structural modeling of the Jeep Indonesia Brand Center showroom building using ETABS software.
4. Carry out calculations and determine dead, live and wind loads with reference to (SNI 1727, 2020) and earthquake loads with reference to (SNI 1726, 2019).
5. Conduct pushover analysis using ETABS software and calculate data using the ATC-40 method and referring to regulations. (SNI 1726, 2019).
6. Evaluation of the structural performance level based on the drift results obtained from the ETABS software according to the ATC-40 method.

7. Make conclusions based on the results of analysis and discussion.

Evaluation of the level of structural performance is carried out based on the results of the pushover analysis. The stages of pushover analysis in this study are as follows (Muntafi, 2012) :

1. Create a nonlinear case in the form of gravity loading and lateral loading as a pushover load in the x and y directions.
2. Modeling and inputting hinge properties data for beam and column elements into ETABS software.
3. Running a pushover analysis program to obtain the building structure performance point from the intersection of the capacity curve and the demand spectrum.
4. Obtain capacity curve data at each step to determine where plastic hinges occur in the building.
5. Conduct evaluations and determine the performance level of building structures by calculating the drift ratio based on the ATC-40 method.

FINDINGS

The structural modeling of the Jeep Indonesia Brand Center Alam Sutera showroom building was carried out in 3D using ETABS software by modeling all elements of columns, beams, plates, and roofs. The results of the building modeling in 3D are shown in Figure 3. The technical data of the building used in the modeling and analysis of the building structure are as follows:

a. Location of the building : Tangerang
b. Building construction : Steel structure
c. Type of building : office and commercial buildings
d. Material specifications
- Profile steel quality : ST-37
- Concrete quality (fc’) : 35 MPa

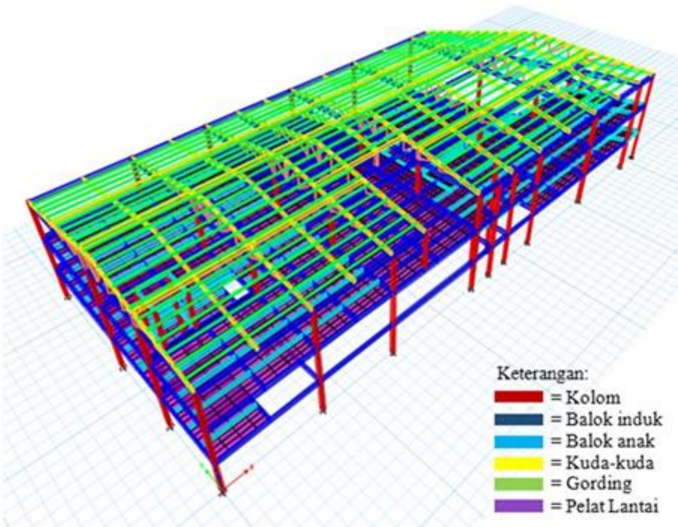

Figure 2. 3D Modeling of Building Structures

A. Earthquake Load Analysis

The static and dynamic base shear force values (base reactions) from the results of the structural analysis due to equivalent static earthquake loading and earthquake response spectrum are shown in Table 2..

Table 2. Basic Static and Dynamic Shear Forces

Output Case	Case Type	FX (kN)	FY kN
SX	LinStatic	-2272.1970	0.0004
SY	LinStatic	-0.0001	-2272.0470
DX Max	LinRespSpec	1215.6586	32.1301
DY Max	LinRespSpec	32.1111	1508.2062

Based on Table 2, the static base shear force value (V) due to equivalent static earthquake load in the x direction = 2272.197 kN and the y direction = 2272.047 kN. While the dynamic base shear force value (Vt) due to the response spectrum earthquake load in the x direction = 1215.6586 kN and the y direction = 1508.2062 kN.

Based on (SNI 1726, 2019) If the dynamic base shear force (Vt) is smaller than the static base shear force (V), then the scale factor must be increased by V/Vt. The calculation of the new scale factor is as follows:

- x – direction scale factor $= \frac{2272{,}197}{1215{,}6585} = 1{,}8691$
- y – direction scale factor $= \frac{2272{,}047}{1508{,}2062} = 1{,}5065$

Then the new scale factor in the x and y directions that have been calculated, multiplied by the previous scale factor by entering it into the ETABS software. After the scale factor is multiplied, then re-analyzed, so that a new dynamic base shear force value is obtained which is greater than the static base shear force shown in Table 3.

Table 3. New Dynamic Basic Shear Force

Output Case	Case Type	FX (kN)	FY kN
SX	LinStatic	-2272.197	0.0004
SY	LinStatic	-0.0001	-2272.047
DX Max	LinRespSpec	2272.2061	60.0548
DY Max	LinRespSpec	48.3742	2272.0576

The deviation between floors must meet the requirements based on Table 20 of SNI 1726:2019 concerning the Deviation Between Permit Levels. Based on the analysis results, the deviation values between floors of the Jeep Indonesia Brand Center Alam Sutera showroom building in the x and y directions have met the requirements and are not more than the deviation values between permit levels shown in Tables 4 and 5.

Table 4. Inter-Floor Deviation X Direction

Lantai	Deviation Direction X (mm)	Delta x (mm)	Delta Permission (mm)	Cek
4	28.098	0.8305	73.75	OK
3	27.947	15.9665	100.00	OK
2	25.044	68.8710	100.00	OK
1	12.522	68.8710	100.00	OK

Table 5. Inter-Floor Deviation Y Direction

Lantai	Deviation Direction X (mm)	Delta x (mm)	Delta Permission (mm)	Cek
4	28.098	0.8305	73.75	OK
3	27.947	15.9665	100.00	OK
2	25.044	68.8710	100.00	OK
1	12.522	68.8710	100.00	OK

Based on Table 4 and Table 5, it is known that the results of the inter-floor deviation for the x and y directions on each floor have met the permitted inter-level deviation (Δ) based on SNI 1726:2019 regulations.

B. Pushover Analysis

The output generated from the pushover analysis is in the form of a capacity curve, performance point, and mechanism of plastic hinge occurrence. The final result of the pushover analysis is in the form of determining the level of building structure performance calculated based on the ATC-40 method. The capacity curve from the results of the pushover analysis in the x and y directions are shown in Figures 3 and 4, respectively.

Figure 3. Curva Capacity Direction X

Figure 4. Curva Capacity Direction Y

The results of the pushover analysis on the pushover loading for the x direction stopped at step 20, namely when the displacement value = 162.741 mm and the base force value = 5522.023 kN. The results of the pushover analysis on the pushover loading for the y direction stopped at step 17, namely when the displacement value = 214.428 mm and the base force value = 10685.072 kN

The determination of the performance point on this building structure uses the ATC-40 capacity spectrum method. This method uses a capacity curve that is converted into the acceleration displacement response spectrum (ADRS) format that shows the relationship between Sa and Sd, as well as a seismic demand curve that is converted into the demand spectrum form (Ertanto et al., 2017). Curve conversion is done automatically in ETABS software. (Riantoby et al., 2014) The performance point is obtained when the capacity curve intersects the spectrum demand curve. After the performance point value is obtained, the drift ratio value can be calculated to obtain the performance level of the building structure by referring to the ATC-40 method. The performance point based on the results of the pushover analysis for the x and y directions can be seen in Figure 5 and Figure 6.

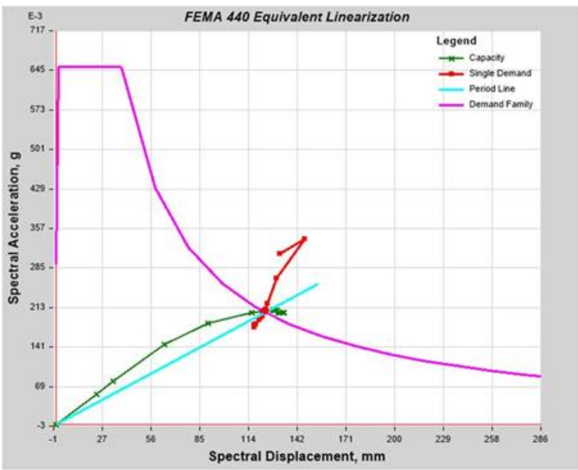

Figure 5. Performance Point in X Direction

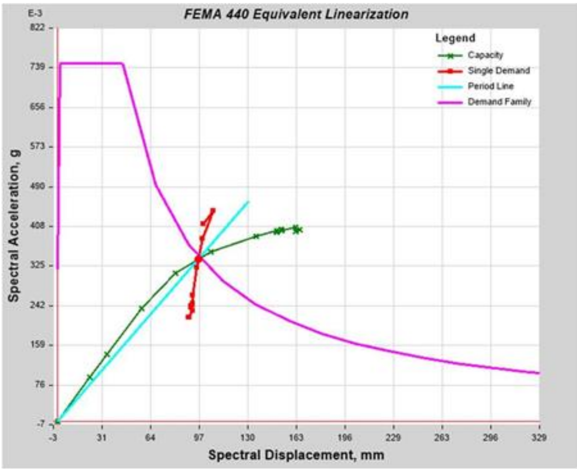

Figure 6. Performance Point in Y Direction

Based on Figure 5 and Figure 6, it can be seen that the capacity curve and demand spectrum have intersected, so that the performance point value can be known. The performance point value from the pushover analysis results in the x and y directions are shown in Table 6.

Table 6. Performance Points from Pushover Analysis Results

Performance Point	Direction X	Direction Y
Point Found	Yes	Yes
Shear (kN)	5577.82	8763.09
Displacement (mm)	151.191	128.285
Sa (g)	0.20784	0.33886
Sd (mm)	123.504	96.16
T secant (sec)	1.546	1.066
T effective (sec)	1.455	1.041
Ductility Ratio	1.81367	1.56279
Damping Ratio, βeff	0.0765	0.0636
Modification Factor, M	0.88518	0.95377

The drift ratio value according to ATC-40 for the maximum total deviation is determined from the comparison between the displacement value at the performance point and the total height of the building. The maximum inelastic deviation is determined from the displacement value at the performance point then reduced by the displacement value at the first step and then compared with the total height of the building. So the drift ratio value for the x and y directions are as follows:

Maximum Total Deviation:

X direction $= \frac{151{,}191}{14950} = 0{,}01011$ (*Damage Control*)

Y direction $= \frac{128,285}{14950} = 0,00858$ (*Immediate Occupancy*)

Maximum Total Deviation:

X direction $= \frac{151,191-29,9}{14950} = 0,00811$ (*Damage Control*)

Y direction $= \frac{192,059-29,9}{14950} = 0,01085$ (*Damage Control*)

From the results of the drift ratio value calculation, it can be seen that the structural performance level of the Jeep Indonesia Brand Center showroom building according to the ATC-40 method is Damage Control (DC), namely the building experienced minor damage due to the earthquake, but the damage can be repaired at an affordable cost and the risk of human casualties is very small. The formation of plastic joints in building structures can be obtained based on the results of pushover analysis. The occurrence of plastic joints based on the results of pushover analysis shown in the ETABS software is marked by the appearance of colored dots on one or more structural elements. Each step of the pushover analysis, there are changes and additions to the plastic joint conditions that occur in the structural elements (Kairatun et al., 2019). Information regarding the occurrence of plastic hinges in structural elements is explained in Table 7.

Table 7. Description of the occurrence of plastic hinges(Marianda, 2016)

Description	Explanation
B	Shows the linear limit that causes an element in the structure to experience the first yielding.
IO	The stiffness of the structure is almost the same as the stiffness before the earthquake, and minor damage that is not significant to the structure begins to occur.
LS	The stiffness of the structure begins to decrease but still has a large enough threshold to reach a state of collapse, and damage begins to occur at a small to moderate level.
CP	The strength of the structure is reduced quite a lot, and quite serious damage to the structure begins to occur.
C	The maximum limit of shear force that can be resisted by a structure
D	The condition of the building became unstable and almost collapsed, and the rigidity of the structure experienced a significant decrease.
E	The collapse of a building occurs due to the inability of the structure to withstand the existing shear force.

In the structure of the Jeep Indonesia Brand Center (JIBC) Alam Sutera showroom building, the pushover analysis stops when there are many structural elements that experience plastic hinges in condition D. The occurrence of plastic hinges based on the results of the pushover analysis in the x and y directions is as follows:

1) Pushover X direction :

The first plastic hinge in the x-direction pushover occurs at step 2 which occurs in the column in condition B shown in Figure 7..

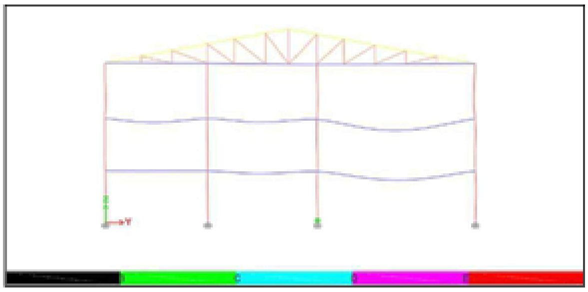

Figure 7. First Plastic Pushover Hinge X Direction in Step 2

Plastic hinges in condition IO begin to occur at step 4 as shown in Figure 9. Plastic hinges in condition C begin to occur at step 6, which is the maximum limit condition for shear force that can be withstood by the structure. Meanwhile, plastic hinges in condition D begin to occur at step 8.

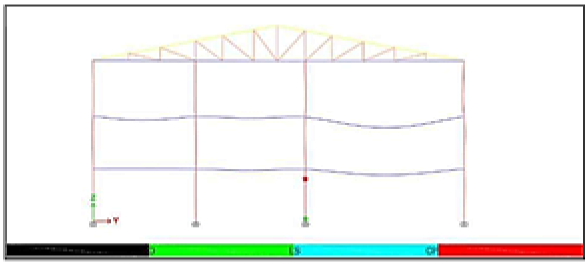

Figure 8. X Direction Pushover Plastic Joint in Step 4

At step 20, there are already many structural components that experience plastic hinge condition D, namely the condition of the building becomes unstable and almost collapses, and the stiffness of the structure experiences a significant decrease. The pushover plastic hinge in the x direction at step 20 is shown in Figure 9.

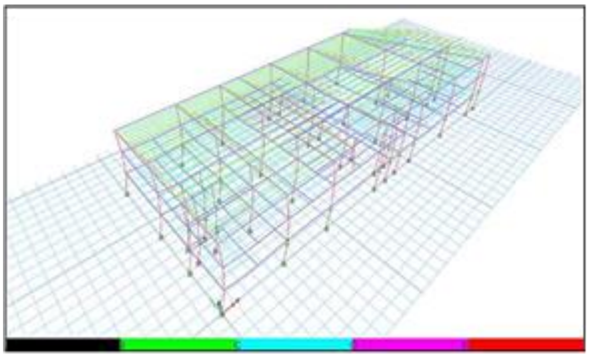

Figure 9. X Direction Pushover Plastic Joint at Step 20

2) Pushover Y direction

The first plastic hinge in the y-direction pushover occurs at step 2 which occurs in the beam in condition B as shown in Figure 10. Meanwhile, the first plastic hinge that occurs in the column occurs at step 3..

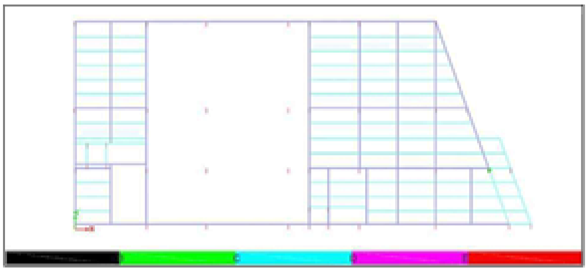

Figure 10. First Plastic Pushover Hinge Y Direction in Step 2

Plastic hinges in condition IO begin to occur at step 5 shown in 11. Plastic hinges in condition C begin to occur at step 7, which is the maximum limit condition for shear force that can be withstood by the structure. Meanwhile, plastic hinges in condition D begin to occur at step 8.

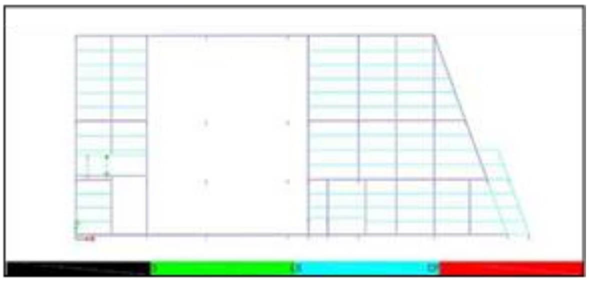

Figure 11. Y Direction Pushover Plastic Joint in Step 4

In step 17, there are already many structural elements that experience plastic hinge condition D, namely the condition of the building becomes unstable and almost collapses, and the stiffness of the structure experiences a significant decrease. The pushover plastic hinge in the y direction in step 17 is shown in Figure 12.

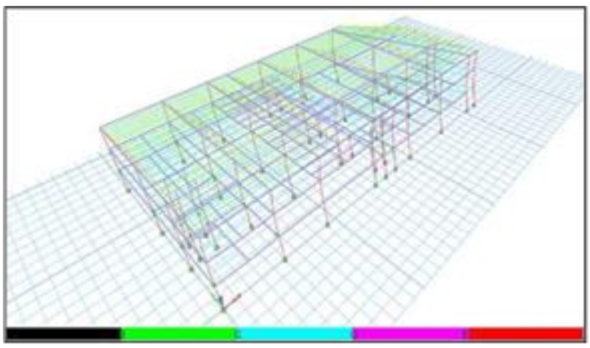

Figure 12. Y Direction Pushover Plastic Joint in Step 17

PRACTICAL IMPLICATION

Based on the performance points obtained, the maximum total deviation value for the x direction = 0.01011 and the y direction = 0.00858. While the maximum inelastic deviation value for the x direction = 0.00811 and the y direction = 0.01085. So that the performance level of the Jeep Indonesia Brand Center (JIBC) Alam Sutera showroom building structure based on the ATC-40 method is Damage Control (DC), namely the building experienced minor damage due to the earthquake, but the damage can be repaired at an affordable cost and the risk of human casualties is very small. The performance of the building structure still meets the requirements according to Table 20 of SNI 1726:2019 which is indicated by the drift value or deviation between floors which is not more than the deviation between permit levels (Δ).

REFERENCES

Aldo, A., & Pratama, G. N. I. (2019). Evaluasi Ketahanan Gempa Rumah Sederhana Di Kelurahan Rum, Kota Tidore Kepulauan. *INERSIA Lnformasi Dan Ekspose Hasil Riset Teknik Sipil Dan Arsitektur*, *15*(2), 1–9.

Choerudin, S. (2008). *Studi Evaluasi Kinerja Struktur Baja Bertingkat Rendah dengan Analisis Pushover*. *Tugas Akhir*. Universitas Kristen Maranatha, Bandung.

Comartin, C. D. (1996). *Seismic evaluation and retrofit of concrete buildings* (Vol. 40). Seismic Safety Commission, State of California.

Dewobroto, W. (2005). Evaluasi Kinerja Struktur Baja Tahan Gempa dengan Analisa Pushover. *Universitas Pelita Harapan*.

Ertanto, B. C., Satyarno, I., & Suhendro, B. (2017). Performance Based Design Bangunan Gedung Untuk Level Kinerja Operasional. *INERSIA Lnformasi Dan Ekspose Hasil Riset Teknik Sipil Dan Arsitektur*, *13*(2), 189–204.

Hakim, R. A. (2013). Seismic assessment of RC building using pushover analysis. *International Conference on Engineering and Technology Development (ICETD)*.

Hakim, R. A., Alama, M. S., & Ashour, S. A. (2014). Seismic assessment of RC building according to ATC 40, FEMA 356 and FEMA 440. *Arabian Journal for Science and Engineering*, *39*, 7691–7699.

Hutama, B. P. (2021). Evaluasi Kinerja Bangunan Rumah sakit Santa Maria Pemalang dengan Non-linier Static Pushover Analysis Metode ATC-40 dan FEMA 440. *INERSIA Lnformasi Dan Ekspose Hasil Riset Teknik Sipil Dan Arsitektur*, *17*(2), 118–129.

Ismaeil, M., Sobaih, M., & Akl, A. (2015). Seismic capacity assessment of existing RC buildings in the Sudan by using pushover analysis. *Open Journal of Civil Engineering*, *5*(2), 154–174.

Kairatun, I., Budiman, E., & Jamal, M. (2019). Analisis Pushover Pada Struktur Baja Dengan Bresing Menggunakan SAP2000. *Teknologi Sipil: Jurnal Ilmu Pengetahuan Dan Teknologi*, *3*(1), 40–49.

Khouy, R., Jiravacharadet, M., & Hoy, M. (n.d.). *SEISMIC PERFORMANCE EVALUATION OF EXISTING RC BUILDING USING BRACED STEEL FRAMES*.

Marianda, D. (2016). *Evaluasi Kinerja Struktur Gedung "Asrama Mahasiswi UGM" Yogyakarta Menggunakan Analisa Pushover Sesuai Pedoman ATC-40*.

Muntafi, Y. (2012). *Evaluasi Kinerja Bangunan Gedung DPU Wilayah Kabupaten Wonogiri dengan Analisis Pushover*.

Nuraga, K., Putri, D. A. P. A. G., Antriksa, K., & Ficher, J. (2021). Analisis Daktilitas Struktur Gedung Rangka Beton Bertulang Dengan Metode Analisis Pushover:(Studi: Gedung Tugu Reasuransi Indonesia Jakarta). *Jurnal Ilmiah Telsinas Elektro, Sipil Dan Teknik Informasi*, *4*(2), 98–105.

Riantoby, I. K., Budi, A. S., & Purwanto, E. (2014). Evaluasi Kinerja Struktur Pada Gedung Bertingkat dengan Analisis Pushover menggunakan Software Etabs (Studi Kasus: Hotel di Wilayah Karanganyar). *Matriks Teknik Sipil*, *2*(1), 116.

Satria, F. A. (2022). *Evaluasi Kinerja Struktur Bangunan Bertingkat Akibat Gempa Berdasarkan Simpangan Dengan Analisis Respon Spektrum (Studi Kasus Apartemen Kingland Avenue Serpong)*.

Scandura, D. (2009). *Physical-Mathematical modeling and numerical simulations of stress-strain state in seismic and volcanic regions*.

SNI 1726. (2019). SNI 1726: 2019 “Tata Cara Perencanaan Ketahanan Gempa Untuk Struktur Bangunan Gedung dan Nongedung.” *BSN, Jakarta, Indonesia*.

SNI 1727. (2020). SNI 1727: 2020 tentang Beban Minimum untuk Perancangan Bangunan Gedung dan Struktur Lain. *Badan Standardisasi Nasional, Jakarta*.

Warsono, W., & Budianto, J. (2019). *EVALUASI KINERJA GEDUNG TERHADAP GAYA GEMPA DENGAN METODE PUSHOVER ANALYSIS Studi Kasus: Pembangunan Gedung Hotel Dan Apartement Gunawangsa Tower A, Gresik, Jawa Timur EVALUATION OF BUILDING PERFORMANCE ON EARTHQUAKE STYLE USING PUSHOVER ANALYSIS METHOD C*. University Technology Yogyakarta.

JACEP

Journal of Applied Civil Engineering and Practices

Online (e-ISSN): e-ISSN XXXX-XXXX || **Printed (p-ISSN)**: p-ISSN XXXX-XXXX
2025, Volume 1, No 1, pp.51 - 65

Analysis of Mobile Crane and Crawler Crane Lift Capacity In Steel Box Girder Type Bridge Construction

Rendy Zaki Musridhoi [a*], **Maris Setyo Nugroho**[a]

[a]Faculty of Vocational Studies, Yogyakarta State University, Yogakarta 55281, Indonesia
[b]Faculty of Engineering, Yogyakarta State University, Yogakarta 55281, Indonesia
*Corresponding Author: rendyzaki.2020@student.uny.ac.id

To cite this article:
Musridhoi, R. Z & Nugroho, M. S. (2025). Analysis Of Mobile Crane and Crawler Crane Lift Capacity in Steel Box Girder Type Bridge Construction. *Journal of Applied Civil Engineering and Practice*, 1 (1), Pp.51-65. doi: xx.xxxx/xxxxxx.xxxx.xxxxxx

To link to this article:
http://doi.org/ xx.xxxx/xxxxxx.xxxx.xxxxxx

2025, Volume 1, No 1, pp.51-65, e-ISSN xxxx-xxxx

Journal of Applied Civil Engineering and Practice

Journal homepage: https://journal.uny.ac.id/publications/jacep/index

Research paper

Analysis of Mobile Crane and Crawler Crane Lift Capacity In Steel Box Girder Type Bridge Construction

Rendy Zaki Musridhoi [a*], Maris Setyo Nugroho [a]

[a]Faculty of Vocational Studies, Yogyakarta State University, Yogakarta 55281, Indonesia
[b]Faculty of Engineering, Yogyakarta State University, Yogakarta 55281, Indonesia
*Corresponding Author: rendyzaki.2020@student.uny.ac.id

ARTICLE INFO

Article History:
Received: March 16, 2025
Accepted: May 2, 2025
Published: 2025

Keywords:
Crane, Erection, Steel Box Girder

How To Cite:
Musridhoi, R. Z & Nugroho, M. S. (202X). Analysis Of Mobile Crane and Crawler Crane Lift Capacity in Steel Box Girder Type Bridge Construction. *Journal of Applied Civil Engineering and Practice*, 1 (1), Pp.51-65. doi: xx.xxxx/xxxxxx.xxxx.xxxxxx

ABSTRACT

Purpose: The causes of work accidents in the erection process are overloading of crane capacity, operational errors, equipment conditions, and planning problems. Operation of a crane that is not in accordance with its capacity has a high chance of causing work accidents. The purpose of this study is to analyze the lifting load, determining the type and capacity of a safe crane, and the bearing capacity of the soil in the crane pad area as an optimization of the box girder steel erection process to improve work safety.

Methods/Design: This research method uses a quantitative descriptive approach. Primary data collection is based on surveys. Secondary data is obtained from testing, project documents, and literature. The independent variables of this study are lifting load, lifting angle, and crane radius.

Findings: In the calculation, the crane lifting load is 126.12 tons divided into 2 tandems so that the load is 63.1 tons. From the analysis of the 250T crane, it is known that the length of the crane boom is 24.4 meters and the working radius is 12 meters with an angle of 65 °, so the lifting capacity of the 250 T crane is 90 tons, with a load capacity rating of 73% and a safety factor of 1.4. While the analysis of the 360T crane, the length of the crane boom is 31 meters and the working radius is 12 meters with an angle of 60 °, so the lifting capacity of the 360T crane is 87 tons, with a load capacity rating of 75% with a safety factor of 1.3. Thus, it has exceeded the ASME 30.5 safety factor standard of at least 1.3.

Practical implication: With the existence of mature calculations related to lifting study cranes, it is hoped that work safety and the success of bridge erection can be improved and construction activities can run efficiently and effectively.

INTRODUCTION

Work accidents during lifting activities during bridge erection using cranes are a serious problem in construction. Lifting crane is the process of using a crane to lift, move, or lower a load. Accidents that occur in this process can be fatal, harming crane operators, workers, and infrastructure. In addition, these accidents can cause major damage to heavy equipment and the load being lifted. According to BPJS Ketenagakerjaan data, work accidents were recorded at 110,285 cases in 2015, decreasing to 101,367 cases in 2016, but increasing significantly thereafter. In 2017, there were 123,040 cases, and in 2018 it jumped to 173,415 cases. In 2019, the number reached 182,835 cases. Since the pandemic in 2020 to 2022, the number of accidents has continued to increase, with 221,740 cases in 2020, 234,270 cases in 2021, and 265,334 cases until November 2022.

The erection process using crane service is high-risk because it involves lifting heavy loads. Erection cranes play a vital role in the assembly and installation of structural elements in construction projects, significantly impacting project timelines, costs, and safety. These cranes are essential for lifting and placing heavy components such as steel structures, precast concrete elements, and large mechanical equipment (Sadeghi et al, 2021). Accidents can occur due to crane overloading or inadequate ground support, such as the Steel Box Girder (SBG) erection project at the Teleng Bridge, which causes land subsidence and increases the risk of accidents. Operator errors, such as incorrect lifting angle settings or damaged equipment, also increase the risk of accidents. Poor planning, inappropriate crane selection, and external factors such as bad weather can worsen the situation, increasing the risk of work accidents.

Despite safety regulations, work accidents often occur due to lack of awareness and understanding of safety in the field. Workers who are not properly trained in K3 procedures can trigger accidents. Accidents can cause losses of material, time, and human resources, even fatalities. The risk increases due to the wide working radius of the crane and the potential for falling or rolling loads. In addition, workers near the crane are also exposed to danger, so protection and safe zones are very important.

Crane lifting operations are critical activities across various industries, including construction, manufacturing, logistics, and ports. The efficiency, safety, and reliability of crane operations directly impact project productivity, operational costs, and the potential for workplace accidents (Zhang & Pan, 2020). Crane lifting activities in erection projects are very crucial and involve heavy equipment and high costs. Selecting the appropriate crane type heavily depends on the characteristics of the load being lifted (weight, dimensions, shape), the conditions of the work site (workspace, ground conditions), and the required reach. Conducts a comparative analysis between various crane types such as crawler cranes, tower cranes, and mobile cranes in the context of high-rise construction projects, considering factors like cost, lifting capacity, and ease of mobilization (Hussein & Zayed, 2021)

Minister of Manpower Regulation No. 38 of 2016 and No. 9 of 2010 emphasize the importance of dividing responsibilities in the Occupational Health and Safety (K3) system, which involves operators, supervisors, and company management. K3 supervisors have an important role in ensuring that heavy equipment operations, such as cranes, comply with safety standards to prevent accidents. Careful and systematic planning is crucial in lifting crane operations, following regulations and technical standards such as the Association Society Mechanical Engineering (ASME) 30.5. In the Teleng Bridge erection project, a lifting study analysis is needed to determine the crane capacity, safe crane types, and the bearing capacity of the soil for the crane foundation, in order to ensure a safe and smooth erection process.

This final project aims to provide solutions to problems in the implementation of Steel Box Girder (SBG) erection on the Teleng Bridge, with a focus on the analysis of lifting loads, safe crane types and capacities, and soil bearing capacity. The goal is to optimize the erection process, prevent land subsidence on the crane pad, reduce the risk of accidents, and improve the smoothness of implementation. The methods used include lifting study analysis and back fill soil bearing capacity analysis.

METHODS/DESIGN

This study uses a quantitative descriptive approach to analyze problems and achieve research objectives by utilizing statistical data. Data is obtained through field observation and testing, then analyzed to produce figures that solve the problems faced, which are the focus of the study. This method was chosen because it is considered the most appropriate for obtaining solutions based on field data that can solve problems during project implementation.

This research was conducted at the Callender Hamilton (CH) Teleng Bridge Construction project, on Jalan Pacitan-Wonogiri, Sidoharjo, Pacitan, East Java. The time interval for implementing this research was carried out from January to July 2023. Data collection was carried out before the analysis to obtain existing data at the project location. This activity was carried out by visiting the CH Teleng Bridge replacement project, Pacitan, East Java.

The data collected is divided into primary data, which is obtained through visits, direct reviews, and testing at the project location. Primary data includes Dynamic Cone Penetration (DCP) and California Bearing Ratio (CBR) value data, Total Steel Box Girder (SBG) weight data. Secondary data includes SBG profile project drawings, embankment work methods, erection work methods, heavy equipment specification data, and Healthy Safety Engineer (HSE) data.

Data analysis is a research stage in the systematic and directed compilation and calculation of quantitative data that has been previously obtained from surveys, field testing, and interviews with related parties as well as sorting and selecting the data needed. Thus, in the end, the implementation and conclusions will be obtained which are expected to be solutions and alternatives for solving problems in the field. The following are research data analysis techniques: (1) Data collection; (2) Data cleaning; (3) Data exploration and organization; (4) Data analysis; (5) Interpretation of results; (6) Decision making; (7) Reporting results; (8) Analysis validation; (9) Reflection, improvement, conclusion.

In the implementation of research, it must be arranged systematically and directed with clear objectives and limitations in accordance with the research method. The following are the stages of implementing this research: (1) Planning includes the preparation of a research design, selection of research subjects, field observations, determination of research objects; (2) Implementation by collecting information through field testing and direct interviews with related parties in the project. This data collection focuses on the Teleng Bridge SBG erection process to optimize the methods used; (3) Data analysis includes justification of work methods, calculation of lifting loads, determination of tools and their capacities, analysis of soil bearing capacity, analysis of lifting studies, erection implementation plans, safety equipment and signs, operator, technician, and rigger checklists, and heavy equipment checklists; (4) Report writing. The erection method with a service crane is a stage of a project that has a relatively large value in the S-curve of work and project budget. With relatively large risks and opportunities for failure. The sanctions received if there is a failure and work accident during the erection process are very large. Therefore, this study was conducted to optimize the method and find alternative solutions related to problems during the SBG with a service crane. The implementation of this study is to optimize the erection method with a service crane so that it is more effective, efficient, and optimal. Thus, it will minimize construction failure and work accidents, especially in erection activities with a tandem service crane method.

FINDINGS

A. Lifting Load Analysis

The calculation of the lifting load from the crane is carried out before the process of determining the type and capacity of the crane. The lifting load consists of the SBG load, the rigging equipment load (sling) and the hook weight (schakle). The lifting procedure using a crane service is contained in the Regulation of the Minister of Manpower of the Republic of Indonesia Number 8 of 2020 concerning Occupational Safety and Health (K3) for Lifting Equipment and Transport Equipment, where the Permenaker standard has a minimum breaking load safety factor standard for the use of rigging. The calculation of the lifting load for the Teleng SBG erection work, Pacitan is in attachment 1. The following is a picture of the SBG Teleng Bridge spanning 60 meters.

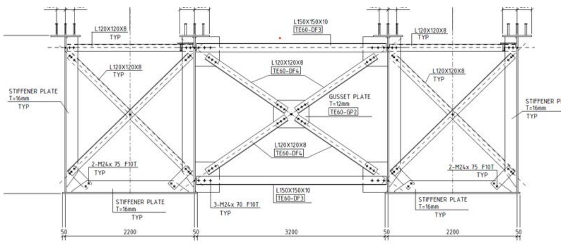

Figure 1. Transverse View of SBG
(Source: Bukaka Teknik Utama)

Based on the lifting load that has been calculated in attachment 1, the total weight on the SBG line 1 is 114.65 tons and the total weight on the SBG line 2 is 112.40 tons. This difference in total weight is due to the difference in the metal deck components installed on the SBG. With the addition of impact load of 10% of the total weight of SBG, the weight of SBG on line 1 becomes 126.12 tons and SBG on line 2 becomes 123.64 tons. Thus, the largest weight is taken for the calculation of crane capacity, which is 126.12 tons. The method used is the tandem method using 1 mobile crane, 1 crawler crane, and 1 set of head tractor with prime over multi axle. Then the weight is divided into 2 tandems so that the weight of each tandem/crane load is 63.1 tons.

Table 1. Additional Load Weight

Rigging	Weight (ton)	Description
Slings	0.300	4 pcs dia. 52 mm IWRC 6x36 *thimble eye*
Shackles	0.092	4 pcs @ 35 T Crosby (tipe g-213)
Master link		
Crane components	1.930	*Capasitas* 160 T *hook block*
Total weight	2.32	Additional burden

The sling on the crane used with the tandem method for both crane 1 and crane 2 is 4 pcs Ø52 mm IWRC 6x36 thimble eye weighing 0.3 tons. While the shackle used is 4 pcs. @ 35 T crosby (Type g-213) weighing 0.092 tons. For the hook block on each crane is installed with a capacity of 160 tons weighing 1.93 tons. Thus the total weight of the sling and shackle per crane is 2.32 tons.

B. Crane Type and Capacity Analysis

Minimum safety factor standards are usually determined based on crane load ratings regulated by standards such as ASME B30.5. This standard provides clear guidelines on the maximum lifting capacity of a crane under various operational conditions, including the weight lifted, distance, and speed of the crane movement. The importance of this calculation is to ensure that lifting operations are carried out safely and in accordance with applicable safety regulations. By complying with the minimum safety factor standards set, the risk of failure or accident during lifting can be significantly minimized.

Table 2. Type of Crane Mounting

Type of Crane Mounting	Max. Load Ratings %
Locomotive, without outrigger support:	
Booms 60 ft (18m) or less	85
Booms over 60 ft (18m)	85
Locomotive, using outriggers fully extended and set	80
Crawler, witout outrigger support	75
Crawler, using outriggers fully extended and set	85
Wheel mounted, without outrigger support	75
Wheel mounted, using outriggers fully extended and set, with tires off supporting surface	85
Wheel mounted, using outriggers beams partially extended and set, with tires off supporting surface	85
Commercial truck vehicle mounted, with outrigger extended and set	85
Commercial truck mounted, using outrigger partially extended and set	85

(Source: ASME. 30. 5)

Selection of the right equipment based on specifications Selection of appropriate equipment based on job specifications and functions will ensure that the work goes according to plan. A 75 T mobile crane is used for the assembly process between 5 box girders with a span of 12 meters into 1 line Steel Box Girder (SBG) with a span of 60 meters. This service crane is a type of crawler crane and does not use outrigger support in lifting activities. So it can be seen that the standard safety factor is 100% divided by 75%. For the results of the safety factor that has been calculated, it produces a safety factor of 1.3% so that the crane is in a safe position. The lifting capacity of the crane can be found using the liftcrane capacities table. Based on the analysis, it is known that the length of the crane boom is 18.3 meters and the working radius of the crane is 6 meters. From this data, the lifting capacity of the service crane is 33,550 tons.

Table 3. Mobile Crane Safety Factor Calculation

Spesification	Value	Description
Boom length	18.30	Meters
Working radius	6.00	Meters
Lifting capacity (d1)	33.50	Tons
Lifting calculation		
Weight of component (a)	24.20	Tons
Lifting point	1.00	Meter from SBG end
Lifting weight (a1)	24.00	Tons
Rigging		
Slings	0.021	4 pcs ø32 mm IWRC 6x36 thimble eye
Shackles	0.078	4 pcs @ 17 T Crosby (tipe g-213)
Master link		
Crane components	1.358	Capasity 50 T hook block
Total weight (b1)	1.46	Tons
Safety Factor Calculation		
Total lift weight (c1) = (a1) + (b1)	25.66	Meters
Lifting capacity (d1)	33.50	Meters
Load capacity rating (e1) = (c1/(d1)	77%	Meters
Safety factor (d1/c1)	1.3	ASME 30.5 min. 1.3 OK

Based on the calculation regarding the crane capacity, it has met the lifting capacity ratio of 77% with a safety factor of 1.3.

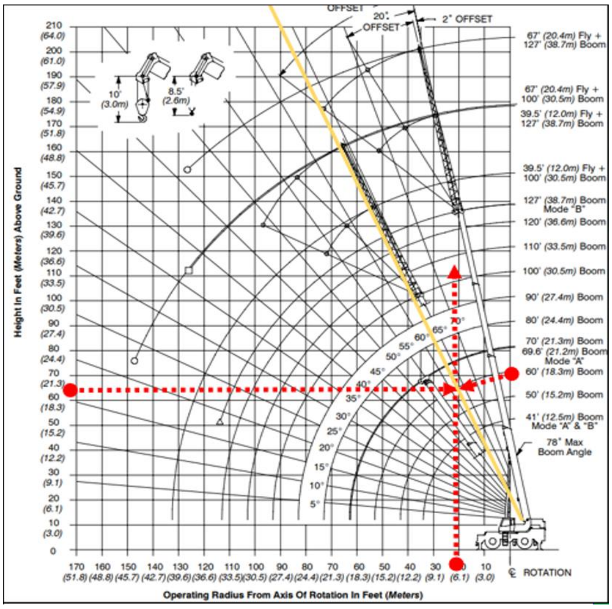

Figure 2. Boom Mobile Crane Service Area
(Source: Crane Market, 2023)

The crane service radius is 6 meters, the boom length is 18.3 meters, based on the graph it can be concluded that the crane service angle is 62.5 °.

The 250T crawler crane is in the abutment area 1. Lifting capacity can be found by looking at the lift crane capacities table as follows with a counterweight of 97.1 tons and a carbody weight of 20 tons. From the analysis of the 250T crane, it can be seen that the length of the crane boom is 24.4 meters and the working radius is 12 meters, so it can be seen that the lifting capacity for the 250 T crane is 90 tons.

According to the lifting plan calculation guidelines, there are two stages to obtain the lifting safety factor calculation, namely the crane safety factor calculation and the sling safety factor calculation. To calculate the crane safety factor, divide the lifting capacity by the total weight for lifting. Based on the calculation in point 1, it is known that the standard safety factor is 1.3% and for the 250T crawler crane, the safety factor is 1.4 so that the crane is in a safe position.

Table 4. Crawler Crane Safety Factor Calculation

Spesification	Value	Description
Boom length	24.40	Meters
Working radius	12.00	Meters
Lifting capacity (d1)	90.00	Tons
<u>Lifting calculation</u>		
Weight of component (a)	126.00	Tons
Lifting point	1.00	Meter from SBG end
Lifting weight (a1)	63.00	Tons
<u>Rigging</u>		
Slings	0.300	4 pcs ø32 mm IWRC 6x36 thimble eye
Shackles	0.092	4 pcs @ 17 T Crosby (tipe g-213)
Master link		
Crane components	1.930	Capasity 50 T hook block
Total weight (b1)	2.32	Tons
<u>Safety Factor Calculation</u>		
Total lift weight (c1) = (a1) + (b1)	65.32	Meters
Lifting capacity (d1)	90.00	Meters
Load capacity rating (e1) = (c1/(d1)	73%	Meters
Safety factor (d1/c1)	1.4	ASME 30.5 min. 1.3 OK

Based on the calculation regarding the crane capacity, it has met the lifting capacity ratio of 73% with a safety factor of 1.4. The following is the crawler crane boom area:

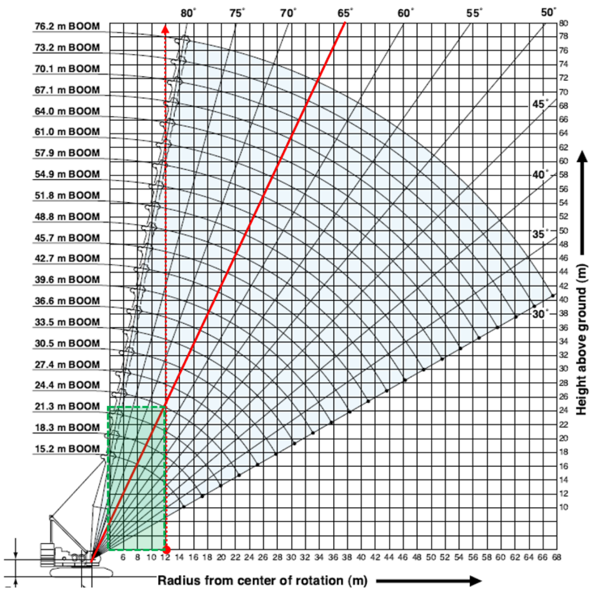

Figure 3. Crawler Crane Boom Area
(Source: Crane Market, 2023)

The radius of the 250 ton crane is 12 meters, the boom length is 24.4 meters, based on the graph it can be concluded that the angle of the 250T crane is 65 °.

The 360T crawler crane is in the A2 abutment area. Lifting capacity can be found by looking at the lift crane capacities table as follows. From the analysis of the 360 ton crane, it can be seen that the length of the crane boom is 31 meters and the working radius is 12 meters, so it can be seen that the lifting capacity is 87 tons.

Table 5. All-Terrain Mobile Crane Safety Factor Calculation

Spesification	**Value**	**Description**
Boom length	31.00	Meters
Working radius	12.00	Meters
Lifting capacity (d1)	87.00	Tons
Lifting calculation		
Weight of component (a)	126.00	Tons
Lifting point	1.00	Meter from SBG end
Lifting weight (a1)	63.00	Tons
Rigging		
Slings	0.300	4 pcs ø32 mm IWRC 6x36 thimble eye
Shackles	0.092	4 pcs @ 17 T Crosby (tipe g-213)
Master link		
Crane components	1.930	Capasity 50 T hook block
Total weight (b1)	2.32	Tons
Safety Factor Calculation		
Total lift weight (c1) = (a1) + (b1)	65.32	Meters
Lifting capacity (d1)	87.00	Meters
Load capacity rating (e1) = (c1/(d1)	75%	Meters
Safety factor (d1/c1)	1.3	ASME 30.5 min. 1.3 OK

Based on calculations regarding the crane capacity, it has met the lifting capacity ratio of 75% with a safety factor of 1.3. The following is the boom area of the all-terrain crane:

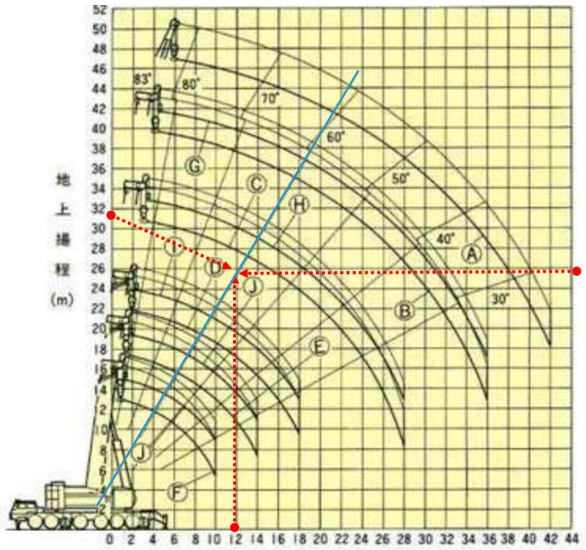

Figure 4. Boom Area of the All-Terrain Crane

C. Lifting Steel Box Girder

The safe capacity of mobile cranes, all terrain cranes and crawler cranes for lifting steel box girders based on the analysis of the lifting study that has been carried out with a total load received by the crane of 65.42 tons is a mobile crane with a capacity of 360 tons and a crawler crane with a capacity of 250 tons. According to the lifting plan calculation guidelines, there are two stages to obtain the lifting safety factor calculation, namely the crane safety factor calculation and the sling safety factor calculation.

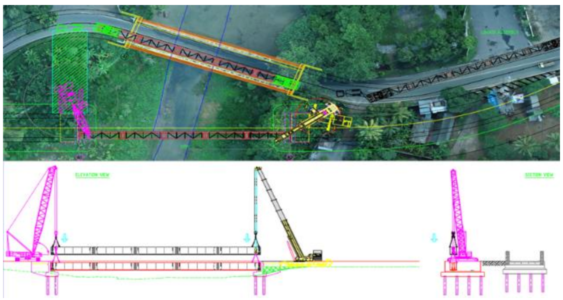

Figure 5. Tandem Method Erection Plan

Based on the calculation, it is known that the standard safety factor based on the maximum load ratings according to the type of crane mounting is 1.3. For a 250-ton crawler crane, it has a lifting capacity of 90 tons and a total load of 65.32 tons, so the lifting ratio is 73% and the safety factor is 1.4. A 360-ton mobile crane has a capacity of 87 tons and a total load received of 65.32 tons, so the lifting ratio is 75% and the safety factor is 1.3. Thus all cranes are in a safe position because they have exceeded the safety factor standard.

D. Analysis of Land Bearing Capacity

Before the equipment for the SBG erection process is mobilized to the location, crane land preparation must be carried out, namely through land filling and compaction. This filling and compaction are important things regarding the success and smoothness of the erection process. The procedure for making crane pads and multi axle pads in the back fill area with fill material for the Teleng Bridge SBG erection is to excavate the soil until a California Bearing Ratio (CBR) of 6% is obtained. Filling with 30 centimeter thick concrete blocks. Filling with 30 centimeter thick limestone compacted to a CBR of 40%.

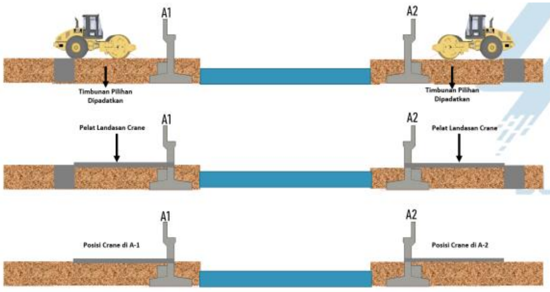

Figure 6. Visualization of Crane Land Preparation Stage

Based on the table of CBR A1 and CBR A2 test results, the CBR test results on land A1, the CBR value of the DCP test results is 45%. The soil density for A1 is 30 tons/m^2. Thus, the soil on land A1 has very good strength, with a CBR value of more than 40% and sufficient density to support the crane load. Then in A1, the CBR value of the DCP test results is 61.5%. The soil density on A2 exceeds 30 tons/m^2, approximately 40 tons/m^2. Thus, the soil on land A2 has good strength, with a CBR value meeting a minimum of 40% and sufficient density to support the use of the crane.

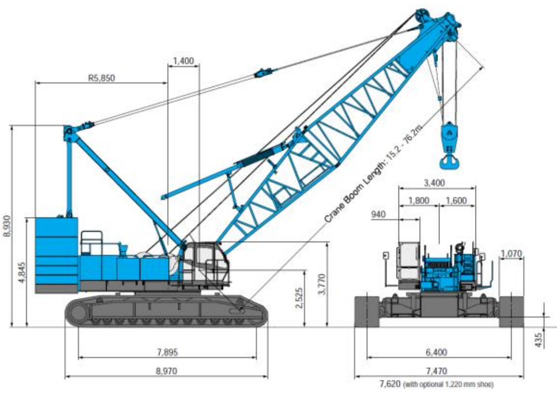

Figure 7. Detailed Specifications of the Kobelco 7250
(Source: Crane Market, 2023)

The crane weighs 211 tons with a lifted load of 63 tons, so the total weight is 274 tons. The runway area is 8.97x7.47, an area of 67.01 m2. The pressure received by the ground is 274 tons divided by an area of 67.01 m2, a value of 4.089 tons/m2. The minimum CBR allowable stress is 40% equivalent to 30 tons/m2 so that the soil supports.

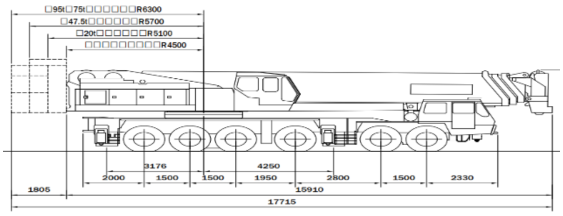

Figure 8. Kato NK3600 Specification Details
(Source: Crane Market, 2023)

The crane weighs 213 tons with a lifted load of 63 tons, so the total weight is 276 tons. The runway area is 11.25x9.2, an area of 104.07 m2. The pressure received by the ground is 276 tons divided by an area of 104.07 m2, a value of 2.652 tons/m2. The minimum CBR allowable stress is 40% equivalent to 30 tons/m2 so that the soil supports.

Table 5. CBR Values GBP Capacity

CBR (%)	GBP *Capacity*		
100	80.74 Psi	551.54Kpa	55Ton/m^2
90	75.28 Psi	514.27Kpa	51Ton/m^2
80	69.62 Psi	475.59Kpa	47Ton/m^2
70	63.71 Psi	435.23Kpa	43Ton/m^2
60	57.51 Psi	392.89Kpa	39Ton/m^2
50	50.95 Psi	348.09Kpa	34Ton/m^2
40	43.94 Psi	300.15Kpa	30Ton/m^2
30	36.29 Psi	247.96Kpa	24Ton/m^2
20	27.73Psi	189.43Kpa	18Ton/m^2
10	17.50 Psi	119.55Kpa	11Ton/m^2

Based on the CBR GBP Cap table, the pressure value received by the soil at abutment 1 is 4.089 tons/m2 and at abutment 2 is 2.652 tons/m2 so it is less than 30 tons/m2 (permissible CBR soil stress) and has exceeded the DCP test value that has been carried out. Thus, the crane runway has met the technical specifications so that the erection process at abutment 1 and abutment can be carried out.

D. Discussion

1. Total weight on SBG line 1 114.65 tons and total weight on SBG line 2 112.40 tons, the difference in total weight is due to the difference in metal deck components installed on SBG. With the addition of impact load of 10% of the total weight of SBG, the weight of SBG on line 1 becomes 126.12 tons and SBG on line 2 becomes 123.64 tons. Thus, the largest weight is taken for the calculation of crane capacity, which is 126.12 tons. The method used is the tandem method using 1 mobile crane, 1 crawler crane, and 1 set of head tractor with prime over multiaxe. Then the weight is divided into 2 tandems so that the weight of each tandem/crane load is 63 tons. The sling on the crane used with the tandem method for both crane 1 and crane 2 is 4 pcs Ø52 mm IWRC 6x36 Thimble eye weighing 0.3 tons. While the shackle used is 4 pcs. @35 T Crosby (Type g-213) weighs 0.092 tons. For Hook block on each

crane is installed with a capacity of 160 tons with a weight of 1.93 tons. The total weight of the sling and shackle per crane is 2.32 tons. Thus the weight received on each crane is 63 tons plus the weight of the sling and shackle 2.32 tons so that the total load is 65.32 tons.

2. Determination of the type and capacity of the crane is influenced by factors, namely the load of the box girder steel and the weight of the sling and shackle of 65.42 tons. The method of SBG erection is influenced by the condition of the erection area where the tandem method is used so that it requires 1 mobile crane and 1 crawler crane. The type of crane installation also affects the crane capacity where the maximum load rating varies according to the type of crane installation. Where the crawler crane does not use outrigger support with a maximum load of 75% and the mobile crane also has a maximum load of 75%. The determination and determination of the boom and crane radius affect the angle taken by the crane and affect the lifting capacity according to the table on the lifting capacity of each crane. The crawler crane has a radius of 12 meters and a boom of 24.4 meters so that the angle is 65° and the lifting capacity is 90 tons. The mobile crane has a radius of 12 meters, a boom length of 31 meters so that the angle is 60° and the lifting capacity is 87 tons.
3. The safe capacity of the mobile crane and crawler crane to transport steel box girders with a total load received by the crane is 65.42 tons is a mobile crane with a capacity of 360 tons and a crawler crane with a capacity of 250 tons. According to the lifting plan calculation guidelines to obtain the lifting safety factor calculation, there are two stages, namely the calculation of the crane safety factor and the calculation of the sling safety factor. To calculate the crane safety factor is to divide the lifting capacity by the total weight lifted. Based on the calculation, it is known that the standard safety factor based on the maximum load rating according to the type of crane installation is 1.3. For a 250-ton crawler crane, it has a lifting capacity of 90 tons and a total load of 65.32 tons, so the lifting ratio is 73% and the safety factor is 1.4. The 360-ton mobile crane has a capacity of 87 tons and a total load of 65.32 tons, so the lifting ratio is 75% and the safety factor is 1.3. Thus, all cranes are in a safe position because they have exceeded the safety factor standard.
4. The amount of soil bearing capacity required for the crane runway is based on a minimum value of 40% or equivalent to 30 tons/m2. The results of the soil DCP test in the abutment 1 and abutment 2 areas respectively obtained values of 45% (32 tons/m2) and 61.5% (40 tons/m2), these values have exceeded the minimum DCP value of 30 tons/m2. The 250-ton crawler crane weighs 211 tons and a lifting load weight of 63 tons, so the total weight is 274 tons. The crawler runway area is 67.01 m2. The pressure received by the ground is 274 tons/67.01 m2 so that it is 4,089 tons/m2. For a mobile crane, it weighs 213 tons and the lifting load weight is 63 tons so that the total weight is 276 tons. The crawler runway area is 104.07 m2. The pressure received by the ground is 276 tons/104.07 m2 so that it is 2,652 tons/m2. Thus, the bearing capacity of the ground has been met.

PRACTICAL IMPLICATION

Based on the results of the research analysis on the analysis of the lifting capacity of mobile cranes and crawler cranes on the construction of steel box girder type bridges that have been carried out, it can be concluded:

1. Based on the calculation of the lifting load of Steel Box Girder (SBG) line 1 is 114.65 tons and the weight of Steel Box Girder (SBG) line 2 is 112.40 tons. The difference in weight occurs due to the difference in metal deck installed above the SBG. The method used is the tandem method using 1 mobile crane, 1 crawler crane, 1 all-terrain crane, 1 set of head tractors including prime over multi-axle. The lifting load per crane plus the weight of the sling and shackle becomes 65.42 tons.
2. Determination and determination of the boom and working radius of the crane affects the determination of the crane angle. The crawler crane has a radius of 12 meters and a boom of 24.4 meters so that the angle is 65o and the lifting capacity is 90 tons. All-terrain crane has a radius of 12 meters and a boom of 31 meters so that the angle is 60o and the lifting capacity is 87 tons.
3. The safety factor value of the crawler crane is 1.4 while the safety factor value of the all-terrain crane is 1.3. Thus all cranes are in a safe position because they exceed the ASME 30.5 safety factor standard with a value of 1.3.
4. The value of the soil bearing capacity on the foundation of the crawler crane and all-terrain crane based on the DCP test is 45% worth 32 tons/m2 and 61.5% worth 40 tons/m2. The value received by the soil due to the crane load and the weight of the crane on the crawler crane and all-terrain crane is 4,089 tons/m2 and 2,652 tons/m2. Thus the soil bearing capacity has been met and the erection process is safe to carry out.

REFERENCES

American Society of Mechanical Engineers. (2021). *Standards B30.5 Mobile and Locomotive Cranes*. https://www.asme.org/

Bukaka Teknik Utama. (2023). *Steel Box Girder Teleng Lifting Study Document*. Pacitan: Bukaka Teknik Utama.

Crane Market. (2024). *Kobelco 7250 and Kato NK3600 Crane Specifications*. https://cranemarket.com/

Minister of Manpower of the Republic of Indonesia. (2016). *Regulation of the Minister of Manpower Number 38 of 2016 concerning Occupational Safety and Health of Power and Production Aircraft*. https://peraturan.bpk.go.id/

Minister of Manpower of the Republic of Indonesia. (2020). *Regulation of the Minister of Manpower of the Republic of Indonesia Number 8 of 2020 concerning Occupational Safety and Health (K3) of Lifting and Transport Aircraft*. https://peraturan.bpk.go.id/

Zhang, H., & Pan, W. (2020). A review of lift planning and optimization in construction. *Automation in Construction*, *114*, 103152. https://doi.org/10.1016/j.autcon.2020.103152

Hussein, A. A., & Zayed, T. (2021). Crane operations and planning in prefabricated construction: A review. *Journal of Building Engineering*, *35*, 102044. https://doi.org/10.1016/j.jobe.2020.102044

Sadeghi, S., Jafari, A., Zayed, T., & El-Sayegh, S. (2021). Analysis of crane risk factors in construction: A literature review and bibliometric analysis. *Safety Science*, *134*, 105078. https://doi.org/10.1016/j.ssci.2020.105078

JACEP

Journal of Applied Civil Engineering and Practices

Online (e-ISSN): e-ISSN xxxx-xxxx || **Printed (p-ISSN)**: p-ISSN XXXX-XXXX
2025, Volume 1, No 1, pp.66 - 78

Analysis of Bored Pile Foundation Bearing Capacity Based on N-Spt Data: (A Case Study of At-Taqwa Mosque Tower Construction Project, Paciran, Lamongan, East Java)

Naufal Kusumawardana [a], **Yuli Fajarwati**[b]

[a]Universitas Negeri Yogyakarta, Department of Civil Engineering, Faculty of Vocational, Indonesia
[a]Universitas Negeri Yogyakarta, Department of Civil Engineering and Planning Education, Faculty of Engineering, Indonesia

*Corresponding Author: naufalkusumawardana.2019@student.uny.ac.id

To cite this article:
Kusumawardana, N. & Fajarwati, Yuli. (2025). Analysis of bored pile foundation bearing capacity based on N-SPT data: (a case study of At-Taqwa Mosque Tower Construction Project, Paciran, Lamongan, East Java). *Journal of Applied Civil Engineering and Practice*, 1 (1), Pp.66-78. doi: xx.xxxx/xxxxxx.xxxx.xxxxxx

To link to this article:
http://doi.org/ xx.xxxx/xxxxxx.xxxx.xxxxxx

Journal of Applied Civil Engineering and Practice by Department Bachelor of Applied Science in Civil Engineering, Faculty of Vocational, Universitas Negeri Yogyakarta.

2025, Volume 1, No 1, pp.66-78, e-ISSN XXXX-XXXX

Journal of Applied Civil Engineering and Practice

Journal homepage: https://journal.uny.ac.id/publications/jacep/index

Research paper

Analysis of Bored Pile Foundation Bearing Capacity Based on N-Spt Data: (A Case Study of At-Taqwa Mosque Tower Construction Project, Paciran, Lamongan, East Java)

Naufal Kusumawardana [a], Yuli Fajarwati[b]

[a]Universitas Negeri Yogyakarta, Department of Civil Engineering, Faculty of Vocational, Indonesia
[a]Universitas Negeri Yogyakarta, Department of Civil Engineering and Planning Education, Faculty of Engineering, Indonesia
*Corresponding Author: naufalkusumawardana.2019@student.uny.ac.id

ARTICLE INFO

Article History:
Received: March 16, 2025
Accepted: May 2, 2025
Published: May 23, 2025

Keywords:

Bored pile, N-SPT, Bearing Capacity

How To Cite:

Kusumawardana, N. & Fajarwati, Yuli. (2025). Analysis of bored pile foundation bearing capacity based on N-SPT data: (a case study of At-Taqwa Mosque Tower Construction Project, Paciran, Lamongan, East Java). *Journal of Applied Civil Engineering and Practice*, 1 (1), Pp.66-78. doi: xx.xxxx/xxxxxx.xxxx.xxxxxx

ABSTRACT

Purpose: The foundation serves as the structural base of a building and is typically located beneath the surface. In this study, the selected foundation type is a bored pile, commonly used in soft soils with low bearing capacity. The choice of bored pile foundations in this project was due to the densely populated surrounding area, making alternative foundation types less feasible. The objective of this research is to evaluate the bearing capacity of bored pile foundations at depths that do not reach the original design plan and to determine the required number of additional bored piles on certain pile caps.

Methods/Design: This study employs a data collection approach, gathering both primary and secondary data. These include soil investigation results (N-SPT data) and bored pile foundation design drawings.

Findings: The data were analyzed to assess the bearing capacity of the bored pile foundation using three methods: Reese & Wright (1977), O'Neil & Reese (1989), and Converse-Labarre (as cited in A'yun, 2022). The analysis revealed the need to increase the number of bored piles from 38 to 45 in order to enhance the total bearing capacity from 2402.33 kN to 3437.81 kN.

Practical Implications: Based on the results of the analysis, the efficiency of the bored pile foundation bearing capacity was found to vary across the three methods: (1) Reese & Wright (1977) yielded 500.28 kN, (2) O'Neil & Reese (1989) yielded 2424.87 kN, and (3) Converse-Labarre (A'yun, 2022) yielded 1778.23 kN. The addition of seven bored piles across the pile caps is considered sufficient in terms of meeting the desired bearing capacity.

INTRODUCTION

In the Journal (Iswati, 2023), soil is the topmost layer of the earth which is formed from particles that have been further processed, due to the influence of air, water and various living and dead organisms. In Indonesia there are many different types of soil, because they have many factors such as volcanoes, coastal areas, hills, and other factors. Indonesia is also an archipelagic country dominated by soft land which reaches around 20 million hectares or around 10% of Indonesia's total land area and is found in coastal areas (Ministry of PUPR, 2002).

In this research location, the project location is located on the seashore and the type of soil at the project location is embankment. The embankment soil is composed of limestone and sand.

The foundation is a strong building base and is usually located below the surface of the land where the building is built (KBBI, 2008:414). The foundation is the lowest structural component of a building which transmits the building load to the soil or rock beneath it (Hardiyatmo, H.C., 2002:79).

The foundation is part of the lower building structure which is divided into 2 groups, namely deep and shallow foundations. Determining the type of foundation depends on whether the superstructure of the building is light or heavy and the type of soil available. Simple building construction usually uses shallow foundations because it has a construction load that tends to be light, while construction of complex buildings usually uses deep foundations because it has a heavy construction load (Hardiyatmo, H.C., 2002:80).

In general, deep foundation types have quite complex structures compared to shallow foundations. Therefore, I tried to concentrate this final project on deep foundations, namely bored pile foundations. Bored piles are used if the soil type is soft soil with low bearing capacity. Choosing a bored pile foundation is more recommended if the surrounding conditions contain high-rise buildings which can cause cracks in the building resulting from pile work (Jusi, 2015). Bored pile foundations, also known as drilled shafts or caissons, are a fundamental type of deep foundation utilized extensively in geotechnical engineering to transfer substantial structural loads through weak or compressible upper soil layers to deeper (Nguyen et all, 2023)

The choice of bored pile foundation was due to the condition around the project being full of residential buildings. In this research, an analysis of the bearing capacity of the bored pile foundation will be carried out to determine its strength and safety based on the results of SPT testing on the At-Taqwa Mosque Tower Construction Project, Paciran, Lamongan, East Java. The Standard Penetration Test (SPT) remains a cornerstone of subsurface soil investigation due to its simplicity, cost-effectiveness, and the extensive empirical correlations it provides for estimating various soil properties crucial for geotechnical design. Carried out within a borehole, the SPT involves recording the number of blows (N-value) required to drive a split-spoon sampler a specific distance into the soil, offering a measure of the soil's resistance to penetration (Prijasambada et all, 2024).

METHOD

This research uses primary and secondary methods. The data used in this research is quantitative and qualitative data. For quantitative data as follows: (1) Standard Penetration Test (SPT); (2)

Boring Log Data. Meanwhile, qualitative data is divided into several items as follows: (1) Literature study; (2) Field observations; (3) Monitoring bored pile; (4) Detailed engineering design; (5) Soil samples.

The analysis was conducted using analytical methods based on established geotechnical engineering principles and empirical correlations, incorporating soil parameters obtained from site investigations. (Sudrajat et al, 2024). Analysis of the bearing capacity of bored pile foundations is carried out after all data has been collected according to field conditions. The data obtained was processed and analyzed to determine the bearing capacity of the bored pile foundation at the At-Taqwa Paciran Mosque Tower project, Lamongan, East Java.

The location of the research was Jl. Raya Dandeles No.164, Paciran, Paciran District, Lamonga Regency, East Java Province.

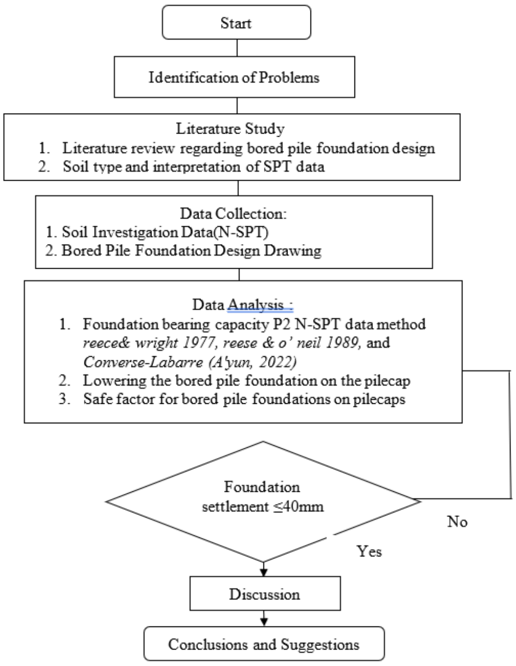

Figure 1. Research Flow Chart

This research was carried out by analyzing the bearing capacity of the foundation which was calculated using the Reece & Wright 1977, O'Neil & Reese 1989, and Converse-Labarre (A'yun, 2022) methods. In this research, the data taken used soil test data (N-SPT), bored pile monitoring data in the field, and planning foundation DED.

Figure 2. *Bored pile* conditions in the field

FINDING

A. Soil Conditions

Soil description from Standard Penetration Test (SPT) drilling results including visual observations of soil type, color and relative soil density. From observations at each drill point, the soil layers at the research location were identified in table 1.

Table 1 BH-01 Point Machine Drill Test Results

Depth (m)	Type of soil/rock
0 – 11.70	Soil filled with limestone mixed with sand with a density level of very loose to medium dense
11.70 – 19.80	Gray clay with a consistency of very soft to very chewy
19.80 – 20.45	Brown Medium Gravel Sand With Loose Density Level
20.45 – 30.00	Fine brown sandy clay with a consistency level of very chewy to hard (UDS 1 at a depth of 9.50m-10.00m)

B. Foundation Plan

The foundation plan in Figure 3 is a picture of the initial planning for the bored pile and pile cap before undergoing any changes. This research takes bored piles which have decreased and added points because in the implementation of bored pile drilling there is a complex problem of the drilling depth factor not reaching the depth planned by the consultant.

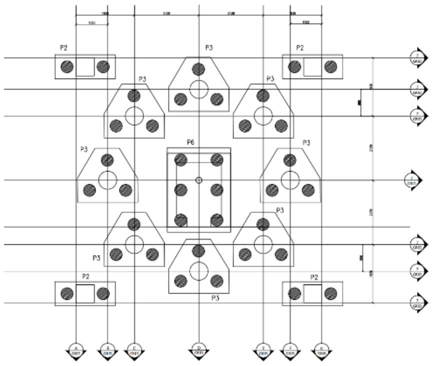

Figure 3. Initial Planning Foundation Plan

C. Data Analysis

1. *Bored pile* specification data

Bored pile specifications used in the At-Taqwa Paciran Mosque Tower construction project, Lamongan are in table 2.

Table 2. Spesifikasi Rencana *Bored Pile*

Description	Information
Bored pile depth(L)	22 m
Ground water level	6 m
Diameter *Bored Pile* (D)	40 cm
Concrete quality (Fc')	30 MPa
Weight of reinforced concrete, (Wc)	24 kN/m^3
Thick concrete cover	5 cm
Quality of reinforcing steel	SNI-TS420B
Diameter of reinforcing steel	- D10 (threaded iron 10 mm) - D16 (threaded iron 16 mm)
Foundation type	*Bored Pile*
Implementation method	Dry and wet drilling methods (using water when drilling)
Type of testing	-

2. Land specification data and N-SPT

Soil specifications and N-SPT bored pile values for the At-Taqwa Paciran Lamongan SPT Mosque Tower construction project are in table 3.

Table 3. Nilai SPT *bored hole*-1

Dept H (m)	N-SPT	N_{60}	γ (kN/m^2)
0	-	-	-
2	15	13.8	19.9
4	12	11.04	19.4
6	12	11.04	19.4
8	6	5.52	15.2
10	10	9.2	15.8
12	4	3.68	18.2
14	2	1.84	17.9
16	3	2.76	18.1
18	25	23	21.4
20	25	23	21.4
22	60	55.2	26.6
24	-	-	-

3. Calculation of the bearing capacity of piles using the *reece & wright 1977* method

In calculating the bearing capacity of the pile using the N-SPT value, using the Reece & Wright 1977 method (Livia & Suhendra, 2018). The ultimate bearing capacity of a single bored pile is stated in equation 16 as follows;

Qu = Qp + Qs (1)

The ultimate bearing capacity at the end of the drilled pile is as follows;

For cohesive soil:

Qp = 9 x Cu x A (2)

Cu = Nspt x 2/3 x 10 (3)

Qp = qp x Ap (4)

Where :

Qp = Bearing capacity of pile tip (tons)

qp = end resistance per unit area (t/m2)

Ap = cross-sectional area of the pole (m2)

For non cohesive soil :

Qp = 7 x N x Ap (5)

The bearing capacity of bored pile blankets is stated as follows;

For cohesive soil :

Qs = α x cu x around the pole x Li (6)

For non cohesive soil :

Qs = 0.2 x Nspt x around the pole x Li (7)

According to Reece & Wright (1977) the value (fs) is oriented to the type of soil and shear strength. For cohesive and non-cohesive soils, you can use the formula equation 15 as follows:

$$f = \alpha \times cu \qquad (8)$$

Where;
α = adhesion factor
cu = soil cohesion (tons/m2)

Reece factor revealed an adhesion value of 0.55. Meanwhile, for non-cohesive values, the f value can be obtained from NSPT. In cohesive soils, q is taken as 9 times the soil shear, the amount of which can be determined based on the Nspt value, while in non-cohesive soils, it is taken as 7 times the soil shear. Reece proposed a correlation of the qp and Nspt values. Based on this formula, planning for the ultimate bearing capacity of a single drilled pile can be used with the following results:

Depth 18 meters with diameter (D) = 0.4 m

Bearing capacity of pile tip

Qp : qp x Ap

Qp : 12.756 x N-SPT

Ap : **0.1256 m^2**

qp : 12.756 x 23.6 => **301.041 t/m^2**

Qp : 301.041 x 0.1256

Qp : **37.81 ton**

Bearing capacity of concrete blanket

Qs : f x L x p (9)

P : π x D => 3.14 x 0.4 = **1.256 m**

f : α x Cu=>0.73 x 9.99 = **7.2927 t/m^2**

Qs : 7.2927 x 20 x 1.256

Qs : **183.17 ton**

Ultimate bearing capacity of single drilled pile

Qu : Qp + Qs

Qu : 37.81 + 183.17

Qu : **220.98 ton**

Depth 18 meters with diameter (D) = 0.8 m

Bearing capacity of pile tip

Qp : qp x Ap

Qp : 10.5 x N-SPT

Ap : 0.5024 m2

qp : 10,5 x 23.6 => **247.8 t/m2**

Qp : 247.8 x 0.5024

Qp : **94.57 ton**

Bearing capacity of concrete blanket

Qs : f x L x p

P : π x D => 3.14 x 0.8 = **2.512 m**

f : α x Cu=>1.4972 x 9.99 = **14,957 t/m2**

Qs : 14.957 x 20 x 2.512

Qs : **156.85 ton**

Ultimate bearing capacity of single drilled pile

Qu : Qp + Qs

Qu : 124.56 + 375.73

Qu : **500.28 ton**

Based on the results of these calculations, the ultimate bearing capacity of a single bored pile using the Reese & Wright 1977 method with a field depth of ±18 meters is Qu = 500.28 tons

4. Calculation of bored pile axial resistance

The calculation of bored pile axial resistance is obtained as follows:

Perimeter of bored pile cross section (P)

P : Π x D (10)

P : 3.14 x 0.40

P : 1.256 m

Bored pile cross-sectional area (Ab)

Ab : $\frac{\pi}{4}\ x\ D^2$ (11)

Ab : $\frac{3.14}{4}\ x\ 0.40^2$

Ab : 0.1256 m^2

Difference between depths (Hi)

Hi : 2 m

Weight *bored pile* (Wb)

Wb : A x L x Wc (12)

Wb : 0.1256 x 18 x 24

Wb : 54.259 kN

Compressive strength of bored pile concrete (fc)

Fc : 33 Mpa

Bored pile nominal bearing capacity (Pn)

Pn : $0.30\ x\ fc'x\ A - 1.2\ x\ Wb$ (13)

Pn : 0.30 x33000 x 0.1256 – 1.2 x 54.259

Pn : 1178.329 kN

Strength reduction factor

(SNI 03 2847-2002), ϕ : 0.60

Axial resistance of piles

ϕ x Pn : 0.60 x 1178.329

: 706.997 kN

5. Calculation of ultimate friction resistance using the reese & o'neil 1989 method

Table 4. Recap of calculation of ultimate friction resistance (Qs)

H (m)	**Qs (kN)**	**∑Qs (kN)**
0	-	-
2	57.7	57.7
4	117.7	175.4
6	234.4	409.8
8	104.4	514.3
10	314.4	828.6
12	341.2	1169.9
14	362.0	1531.9
16	373.4	1905.2
18	380.5	2285.7
20	382.0	2667.8
22	379.1	3046.8

Calculation of ultimate bearing capacity using the reese & o'neil 1989 method

Uplift (U)

$$U : A \times (L - MAT) \times \gamma wa \tag{14}$$

$$U : 0.1256 \times (22 - 6) \times 10$$

$$U : 20.096 \text{ kN}$$

Bored pile weight due to uplift (Wb')

$$Wb' : Wb - U \tag{15}$$

$$Wb' : 54.259 - 20.096$$

$$Wb' : 34.163 \text{ kN}$$

Ultimate bearing capacity (Qu)

$$Qu : Qb + \sum Qs - Wb' \tag{16}$$

$$Qu : 173.328 + 2285.7 - 34.163$$

$$Qu : 2424.865 \text{ kN}$$

Ultimate support capacity (Qall)

$$Qall : Qu/sf \tag{17}$$

$$Qall : 457.615/2.5$$

$$Qall : 1010.36 \text{ kN}$$

So the permit carrying capacity for the At-Taqwa Paciran Lamongan Mosque Tower construction project using the O'Neil & Resse 1989 method obtained is 1010.36 kN.

6. Calculation of the efficiency of the pile bearing capacity using the *converse-labarre (A'yun, 2022)* method

Table 5. Pile bearing capacity efficiency (Qg)

No.	Story	Joint	N (piece)	Qg (kN)
1.	BASE	9	2	1778.23
2.	BASE	15	2	1778.23
3.	BASE	17	3	2546.10
4.	BASE	20	3	2546.10
5.	BASE	24	3	2546.10
6.	BASE	51	3	2546.10
7.	BASE	56	3	2546.10
8.	BASE	75	3	2546.10
9.	BASE	79	3	2546.10
10	BASE	82	3	2546.10
11.	BASE	84	2	1778.23
12.	BASE	90	2	1778.23
13.	SW		6	4061.64

From table 5, it can be seen that the number of bored pile poles required for initial planning is seen from the efficiency value so that the required number of poles for each pile is obtained. After that, the bored pile point is added to the specified pile cap so that the results of the bearing capacity calculation in the field are obtained in table 6.

Table 6. Requirements for the number and carrying capacity of bored piles in the field

No.	Story	Joint	Number of poles (n) (peice)		Qg (kN)
1.	BASE	9	2.05	3	2546.10
2.	BASE	15	2.02	2	1778.23
3.	BASE	17	2.99	4	2829.008
4.	BASE	20	3.06	4	2829.008
5.	BASE	24	3.01	4	2829.008
6.	BASE	51	2.91	4	2829.008
7.	BASE	56	2.83	3	2546.10
8.	BASE	75	3.02	3	2546.10
9.	BASE	79	2.97	3	2546.10
10	BASE	82	2.98	3	2546.10
11.	BASE	84	2.02	2	1778.23
12.	BASE	90	2.00	2	1778.23
13.	SW		5.81	8	5334.70
			Total =	**45**	

D. Discussion

The implementation of bored pile work on the At-Taqwa Paciran Lamongan Mosque Tower construction project in the field did not go smoothly as planned. There are unexpected deviations from previous plans, resulting in obstacles/problems that need to be readjusted. Some of these obstacles include:

The drill bit was unable to penetrate the rock, which resulted in the drilling not reaching the planned bored pile depth target of 22 m, so the depth reached was at a depth of 18 m.

The cast concrete does not match the quality of the concrete, namely K350. There are several tests where the compressive strength does not meet the quality of the concrete.
1. Comparison of planned and field bored pile carrying capacity
After calculating the carrying capacity for conditions in the field, a comparison of the planned and field carrying capacity values is carried out as follows:

Table 7. Comparison of the planned bored pile carrying capacity with the field

Description	Unit	Plan	Field
Weight, Wb	kN	66.317	54.259
Pn	kN	1163.86	1178.329
Axial resistance	kN	698.316	706.997
As	m^2	2.512	2.512
z	m	21	17
β		0.38	0.49
po’	kN/m^2	53.2	42.8
Σpo’	kN/m^2	426.6	330.6
Po’ average	kN/m^2	400	309.2
Qs	kN	379.1	380.5
ΣQs	kN	3046.8	2285.7
Qu	kN	3416.59	2424.865
Qall	kN	1366.64	1010.36

Based on table 7, after the addition of bored pile points, there is an increase in the value of axial resistance and the carrying capacity of the planned bored pile permit (Qall) with the field. Initially the planned axial resistance was 698.316 kN, increased to 706.997 kN. The same thing happened to the permit carrying capacity (Qall), which increased with a value of the difference between the two of 356.28 kN.

This shows that differences in depth factors (H) and concrete quality (fc') can significantly influence the bearing capacity of bored pile foundations.

1. Requirements for the number and efficiency of field bored pile pile bearing capacity
Calculation of the efficiency of bored pile carrying capacity in field conditions using different methods, so that the number of bored pile piles needed is known in terms of the carrying capacity efficiency value in table 8.

Table 8. Requirements for the number and efficiency of field bored pile carrying capacity

No.	Story	Joint	Number of poles (n) (piece)		Qg (kN)	Qg > P
1.	BASE	9	2.05	3	2546.10	OKE
2.	BASE	15	2.02	2	1778.23	OKE
3.	BASE	17	2.99	4	2829.008	OKE
4.	BASE	20	3.06	4	2829.008	OKE
5.	BASE	24	3.01	4	2829.008	OKE
6.	BASE	51	2.91	4	2829.008	OKE
7.	BASE	56	2.83	3	2546.10	OKE
8.	BASE	75	3.02	3	2546.10	OKE
9.	BASE	79	2.97	3	2546.10	OKE
10	BASE	82	2.98	3	2546.10	OKE
11.	BASE	84	2.02	2	1778.23	OKE
12.	BASE	90	2.00	2	1778.23	OKE
13.	SW		7.81	8	5334.70	OKE
			Total =	**45**		

From Table 8 it is known that the total number of bored piles needed in the field is 45 points, each of which has met its carrying capacity efficiency. This condition shows the addition of 7 points from 38 pile points to 45 pile points. This occurs due to differences in the bearing capacity of bored piles in field conditions due to changes in depth and quality of concrete.

4. Conclusion

Based on the calculation results of the bored pile foundation planning for the At-Taqwa Paciran mosque tower construction project, Lamongan, East Java, several conclusions can be drawn as follows:

1. Calculation of the efficiency of bored pile bearing capacity in field conditions using different methods by adding 7 bored pile points to 45 points to increase the bearing capacity of the P2 pile cap by 1778.23 kN to 2546.10 kN. Calculation of the efficiency of bored pile carrying capacity in field conditions using the same method, so that it is known that the required number of bored pile piles in terms of the carrying capacity efficiency value is sufficient.

2. Addition of the number of bored pile points to each pile cap that has been determined is 7 points.

3. The bearing capacity of the bored pile foundation at a depth of 18 m using the Reese & Wright 1977 method is 500.28 kN, O'Neil & Reese 1989 is 2424.865 kN, and Converse-Labarre (A'yun, 2022) is 1778.23 kN.

REFERENCE

Iswati, R. K. (2023). *Comparative analysis of the carrying capacity of bored pile foundations based on N-SPT and PDA test data for the Kasih Ibu Hospital Building Construction Project, Surakarta* [Undergraduate thesis, Bangun Nusantara University]. Retrieved from https://eprints.univetbantara.ac.id/id/eprint/14

Ministry of PUPR. (2002). *Formation process and basic properties of soft soil geotechnical guide I*. Department of Settlements and Regional Infrastructure.

Jusi, U. (2015). *Analisa Kuat Dukung Pondasi Bore Pile Berdasarkan Data Pengujian Lapangan (Cone and N-Standart Penetration Test)* [Skripsi tidak diterbitkan]. Sekolah Tinggi Teknologi Pekanbaru. https://www.researchgate.net/publication/332068327

Livia., & Suhendra, A. (2018). Drilled pile capacity study based on the Pile Driving Analyzer (PDA) and Load Cell Method. *Civil Engineering Partner Journal*. Retrieved from https://journal.untar.ac.id/index.php/jmts/article/view/2245/1301

Sudrajat, K. M., Jumantoro, I., Isradi, M., Prasetijo, J., Rifai, A. I., & Sobirin, M. (2024). Analysis of Bearing Capacity of Bored Pile Foundation: Case Study of Jakarta – Bandung Station, Karawang High-Speed Railway. *European Journal of Science, Innovation and Technology*, *4*(4), 145-161. Retrieved from https://ejsit-journal.com/index.php/ejsit/article/view/499

Nguyen, T. T., Le, T. A., & Bui, T. Q. (2023). Sustainable design and optimization of pile foundations using metaheuristic algorithms. *Applied Sciences*, *13*(3), 1487.

Prijasambada, P., Tunafiah, H., & Natadipura, R. K. (2024). Analysis of Bearing Capacity of Bored Pile Foundation: Case Study of Jakarta – Bandung Station, Karawang High-Speed Railway. *European Journal of Science, Innovation and Technology*, *4*(4), 145-161. https://ejsit-journal.com/index.php/ejsit/article/view/499